中核集团 CNNC
核工业西南物理研究院
Southwestern Institute of Physics

Physical Experiments of Heating and Current Drive in Fusion Plasmas

Min Jiang

Southwestern Institute of Physics (SWIP)

15th ITER International School, 20-24/07/2026, Leshan, China

How do we experimentally know that a H&CD system has truly achieved the intended physical effects?

- How to use H&CD in real experiments?
- How to diagnose their effects?
- How H&CD influences plasma performance?

Outline

- Physical requirements for H&CD
- Overview of H&CD systems from experimental view (actuator)
- Measurements of H&CD (measurement)
- Application in fusion experiments (plasma response)
  - Profiles control and transport study
  - H-mode access
  - Fast-ion physics
  - Integrated control and scenario optimization
- Summary

Outline

- Physical requirements for H&CD
- Overview of H&CD systems from experimental perspective
- Measurements of H&CD
- Application in fusion experiments
  - Profiles control and transport study
  - H-mode access
  - Fast-ion physics
  - Integrated control and scenario optimization
- Summary

Heating is necessary for fusion

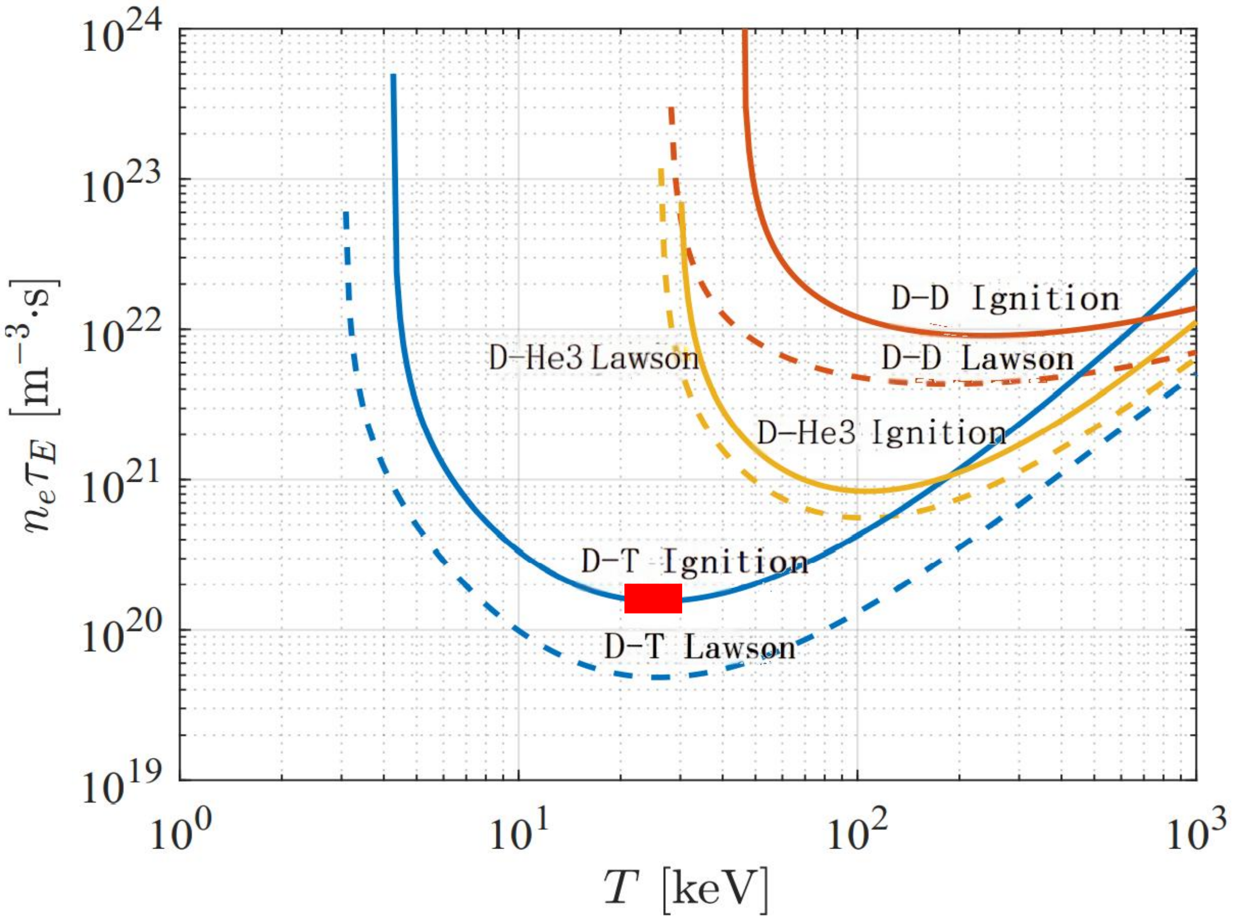

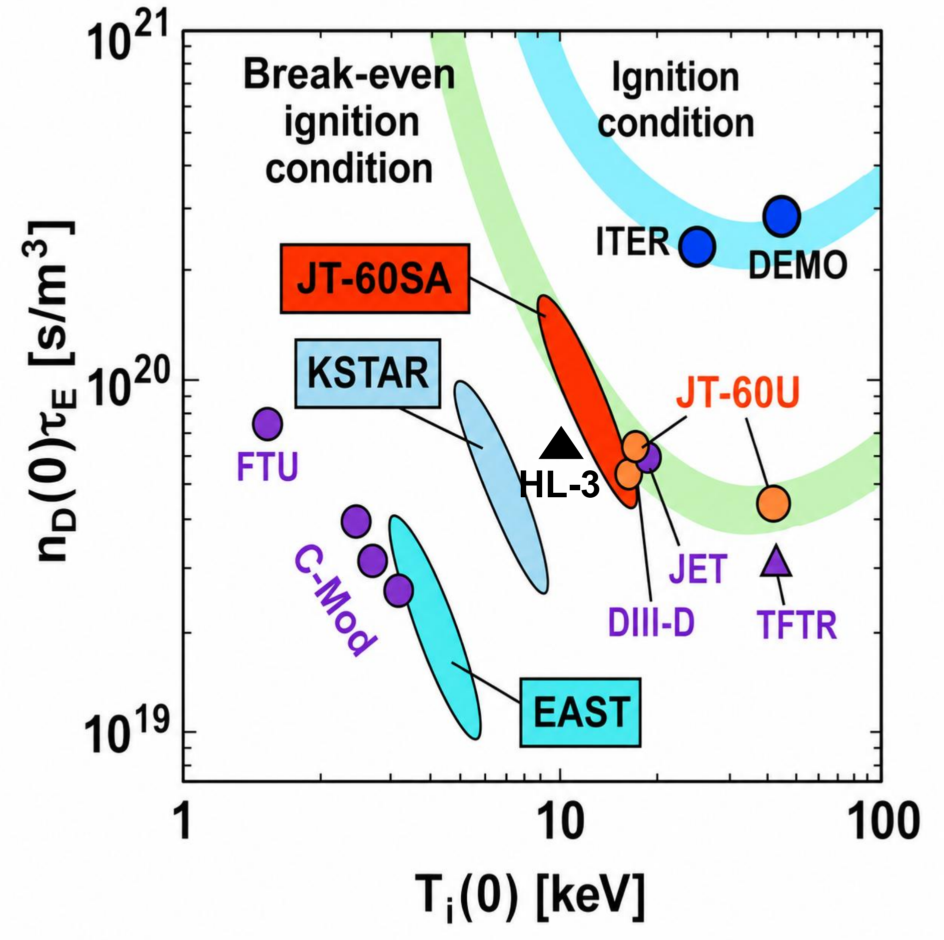

For D-T ignition: $n_e\tau_E T_i \geq 3\times10^{21}\ keV\cdot m^{-3}\cdot s$ **(Lawson criteria)**

$n_e\tau_E \geq 1.5\times10^{20} m^{-3}\cdot s$ **@ T~20-30 keV**

Why do we need auxiliary heating?

- Ohmic heating cannot **heat the plasma to the transition temperature** for ignition unless a very high magnetic field of 15-20 T is available (economically).

  Rough estimation:

  $P_\Omega = I^2 R \propto B^2/T^{3/2}$ (rapidly decreasing with T↑)

  $nT/\tau_E = P_\Omega \rightarrow T^{5/2} \propto \tau_E B^2 \propto B^{2\text{-}4}$

  (depending on the scaling law of τ_E)

- Additional heating techniques needed to obtain 15-20 keV.

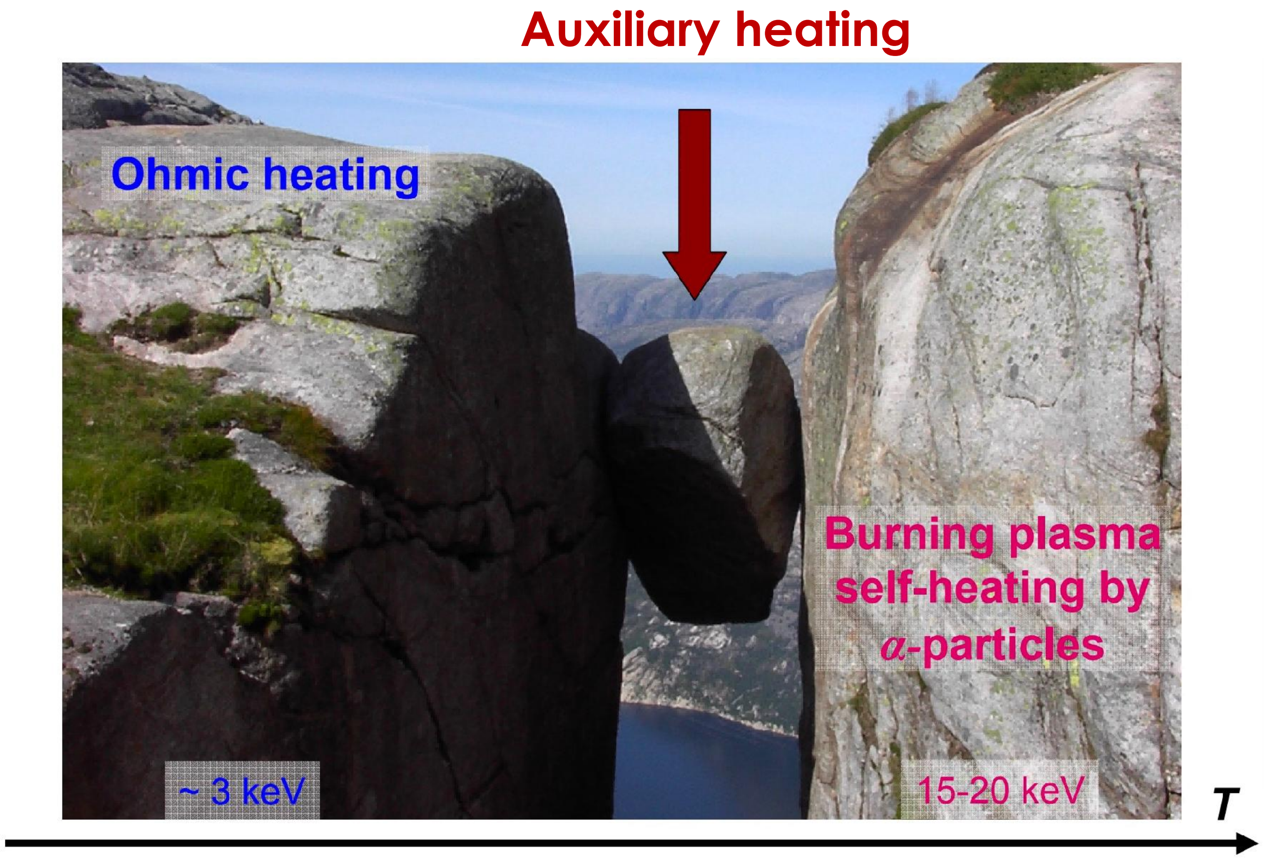

Why do we need non-inductive CD in tokamaks?

Plasma current in tokamaks is essential for confinement, equilibrium and stability.

Inductive current is limited

- Transformer-driven
- Finite magnetic flux swing
- Intrinsically pulsed

Current drive enables

- Long-pulse/steady-state operation
- Current profile control
- Advanced scenarios
- MHD stabilization

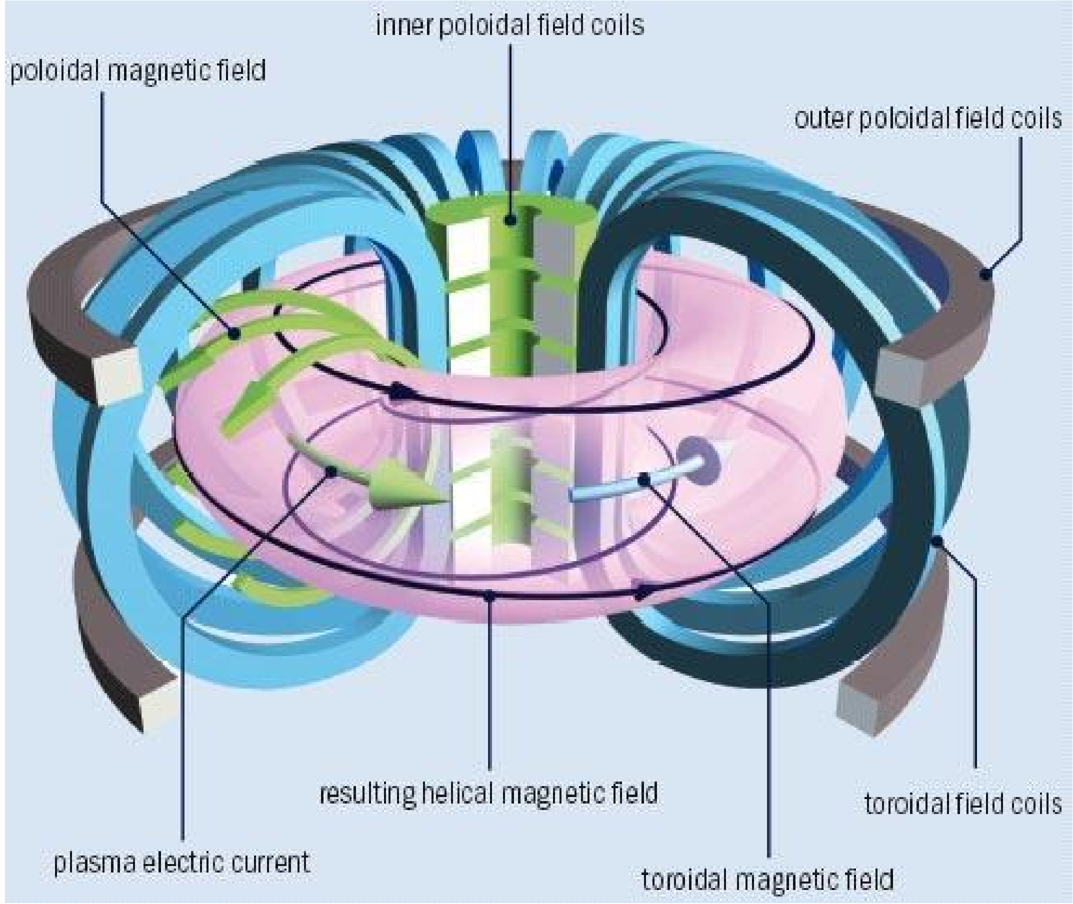

H&CD as a control system

H&CD → Te(r), Ti(r), ne(r), q(r), Vφ(r) → Turbulence, Transport, MHD stability, confinement → Steady-state, high performance advanced scenario

H&CD systems are more than power injection or current source, they are also plasma actuators for transport and confinment, scenario development, and MHD control, etc.

Outline

- Physical requirements for H&CD
- **Overview of H&CD systems from experimental perspective**
- Measurements of H&CD
- Application in fusion experiments
  - Profiles control and transport study
  - H-mode access
  - Fast-ion physics
  - Integrated control and scenario optimization
- Summary

Main H & CD methods in fusion devices

Heating Scheme	Absorbing Particles	Limitations
Ohmic Heating	Electrons	Temperature~2-3keV,can't reach ignition condition
NBI	Ions and Electrons	MeV beam energy needed for reactor relevant high densities
ICRH	Ions and Electrons	Antenna close to plasma, Coupling, Impurities, RF sheath
ECRH	Electrons	Cut-off Densities, Sensitivity to alignment
LHCD	Electrons	Antenna close to plasma, Impurities, off-axis heating only
Alpha particle	Ions and Electrons	20% of total fusion power

All medium and large-size tokamaks and stellarators have a mix of these heatings; also ITER.

Main H & CD methods in fusion devices

NBI: Heat ions, Fast-ion and momentum sources.

ECRH: Locally heat electrons, and provides ECCD, sawtooth/NTM stabilization, plasma start-up assistance.

LHCD: Off-axis current drive, advanced scenarios, long pulse steady-state operation

ICRF: Couple power to high density plasmas and plasma core, MeV fast-ion sources.

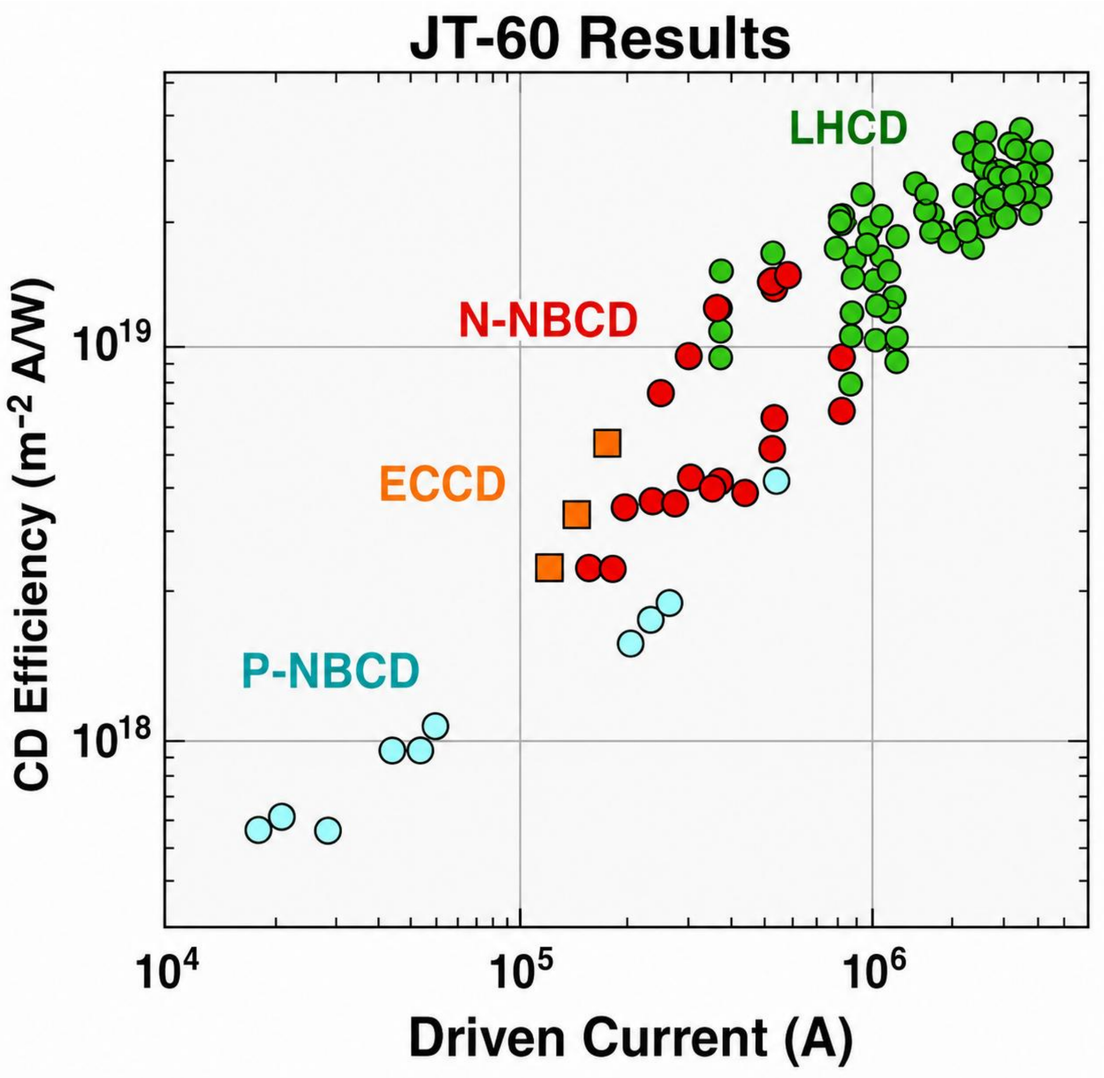

Outline

核工业西南物理研究院 Southwestern Institute of Physics 中核集团 CNNC

- ☐ Physical requirements for H&CD
- ☐ Overview of H&CD systems from experimental perspective
- ☐ **Measurements of H&CD**
- ☐ Application in fusion experiments
  - ➢ Profiles control and transport study
  - ➢ H-mode access
  - ➢ Fast-ion physics
  - ➢ Integrated control and scenario optimization
- ☐ Summary

How to measure H&CD experimentally?

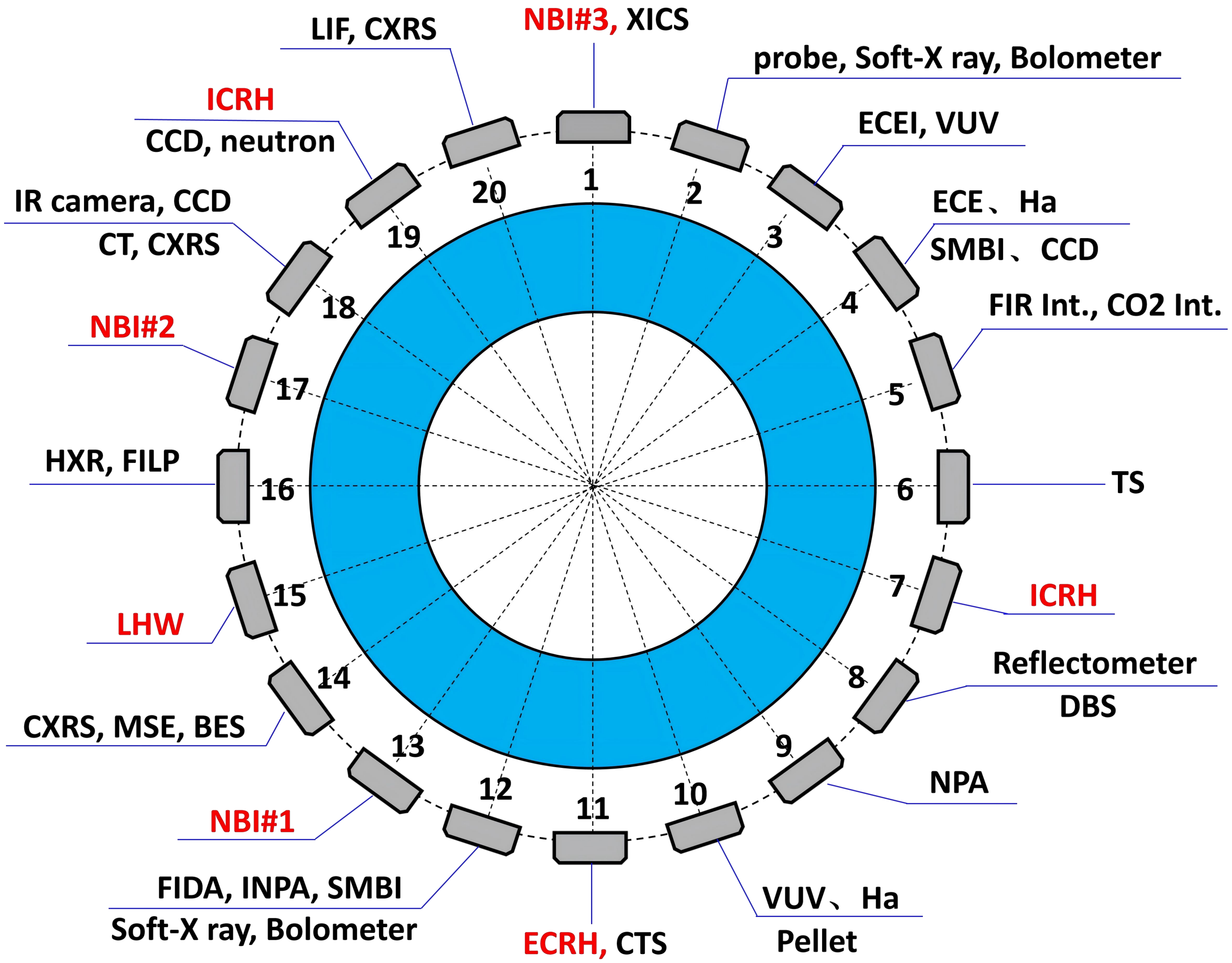

Electron temperature (T_e) measurement

Thomson scattering

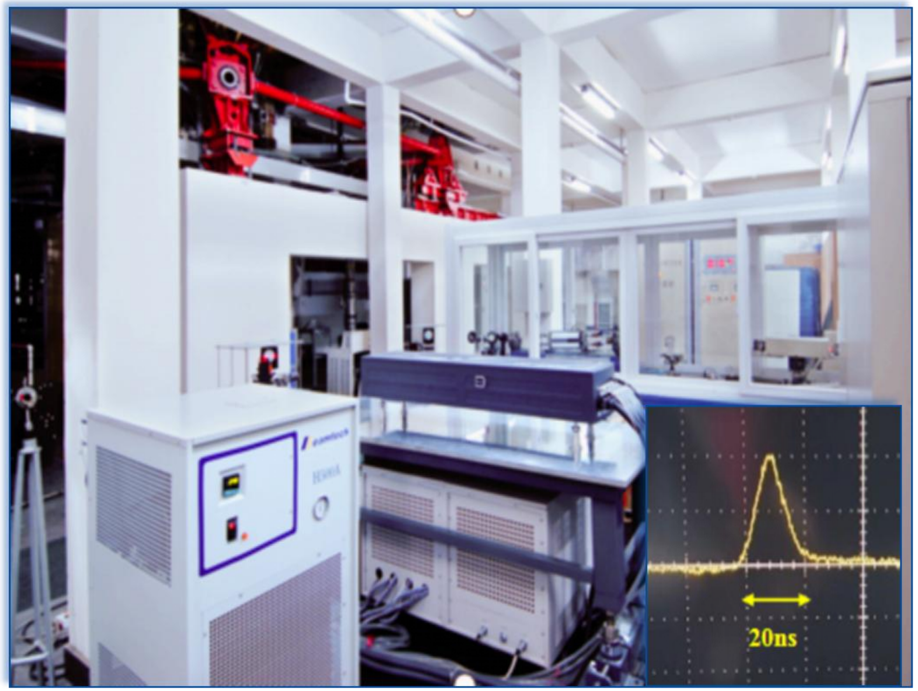

HL-3 TS

	参数
λ	1064 nm
f/Δt	30 Hz/33 ms
Energy	2.0 J
Δl	15 mm
FOV	0<r/a<1.1
Channels	**>60**
Te	**10eV-15 keV**
Ne	**>5×10^{18} m^{-3}**

Electron cyclotron emission

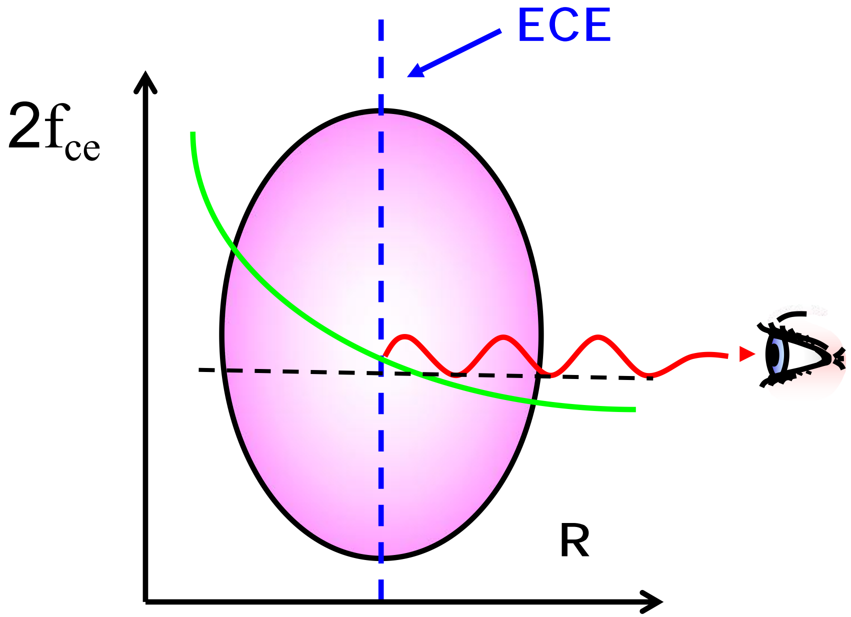

$$\omega = \frac{n_e B_0 R_0}{\gamma m_e R}$$

2nd X-mode ECE: I_{ECE}=CT_e

Resolution: 2 μs, 1 cm

Ion temperature (T_i) and rotation (V_Φ) measurement

Charge exchange recombination spectroscopy (CXRS)

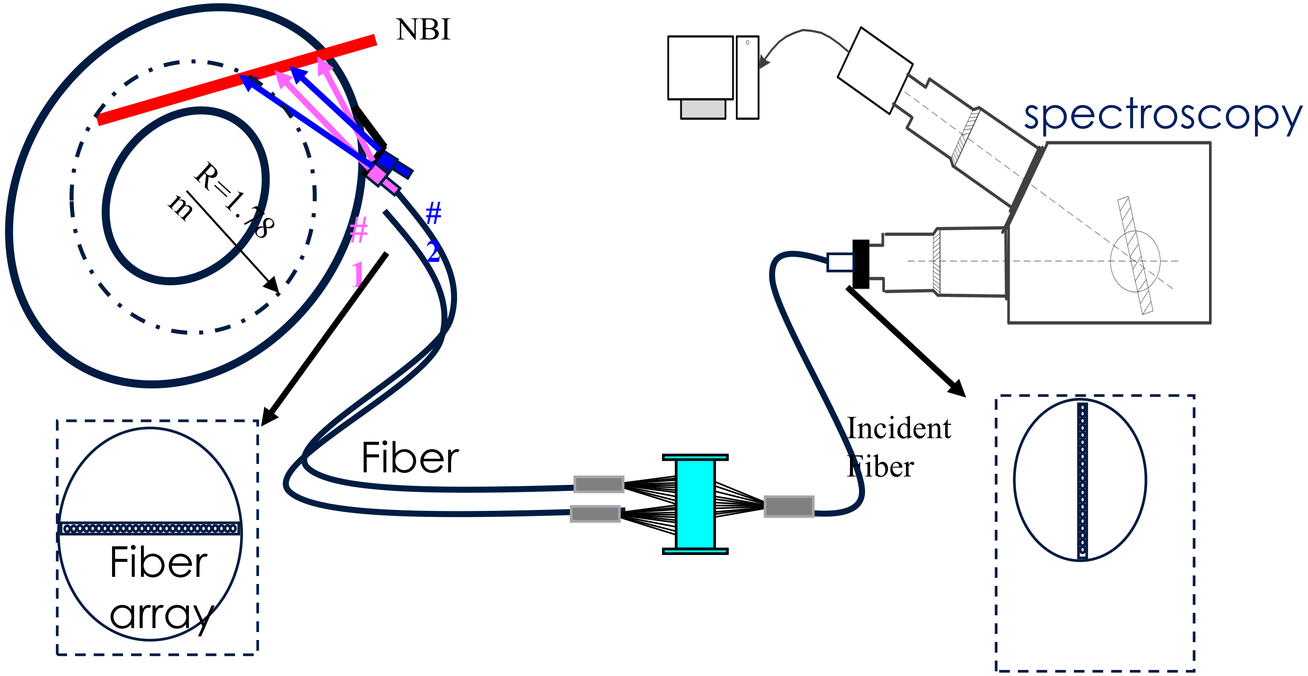

- T_i and V_Φ: From Doppler broadening and shift
- Resolution: 2cm，5-50 ms;
- Color dispersion rate: 0.0117nm/pixel @529.05nm

X-ray Imaging Crystal Spectrometer (XICS)

- T_i and V_Φ
- Resolution: 20ms / ~1.5cm
- wavelength: 3.94-4.01Å ,
- Spectral line: 3.9494Å (Ar XVII *w*-line)

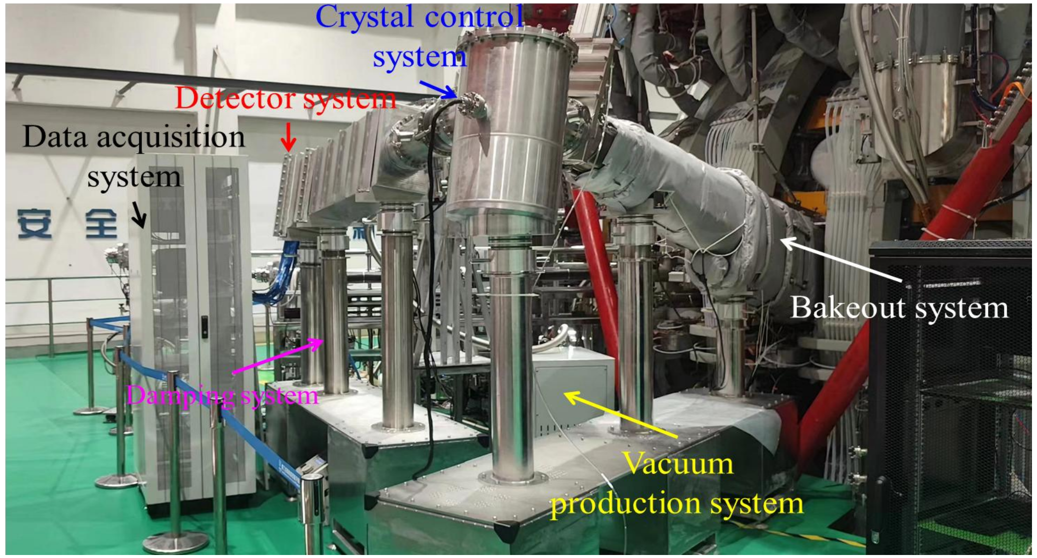

Current profile

FIR/THz Polarimeter

Faraday angle: $\alpha_F(x) \propto \lambda^2 \int n_e B_Z \, dz$

resolution: 0.1°, 1–100 μs

Polarimeter+EFIT → $J_\Phi(r)$

JET

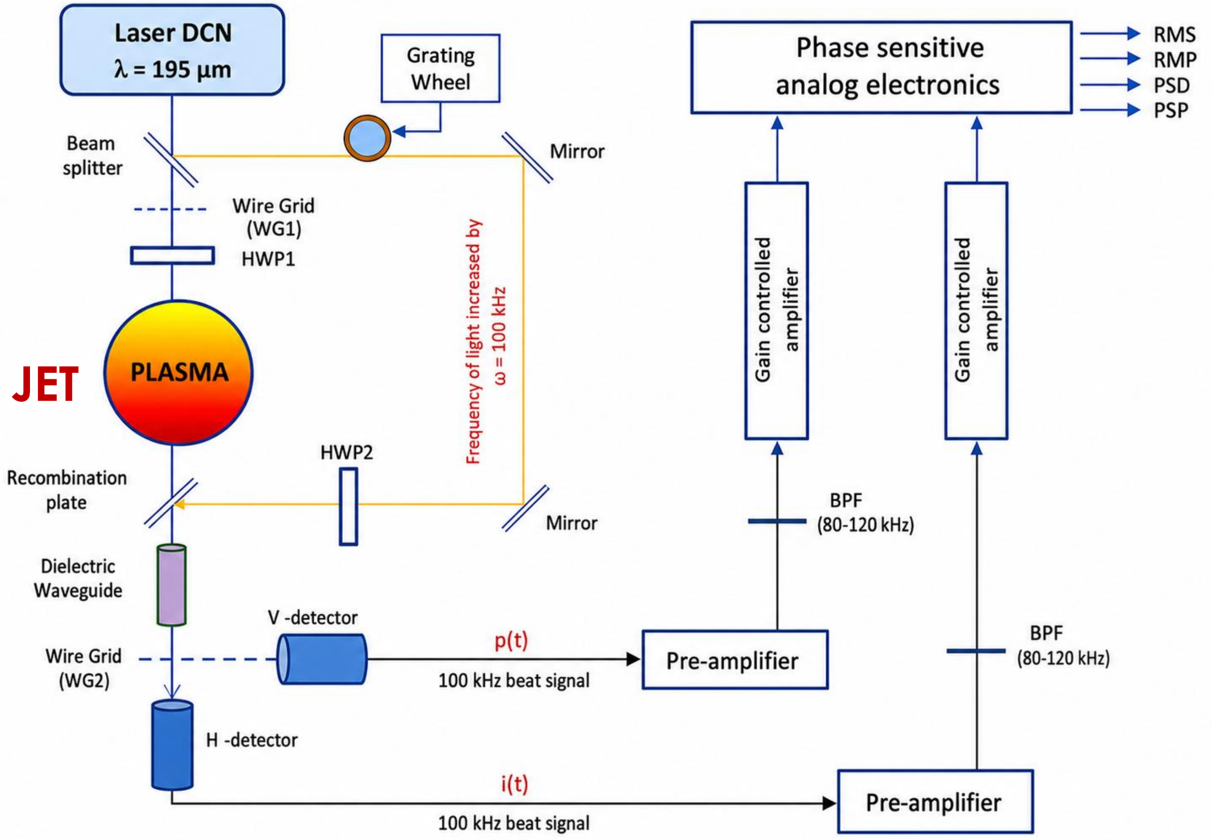

Motional Stark Effect (MSE)

λ_0≈656.1 nm (D_α), π /σ Component

Local: $\tan\gamma \propto \frac{B_\theta}{B_\phi}$ $q(r) \simeq \frac{rB_\phi}{RB_\theta}$

Resolution: 1-3 cm, 1 ms

MSE+EFIT → $J_\Phi(r)$

MSE Viewing Geometry For Simultaneous q and E_r Measurements

DIII-D

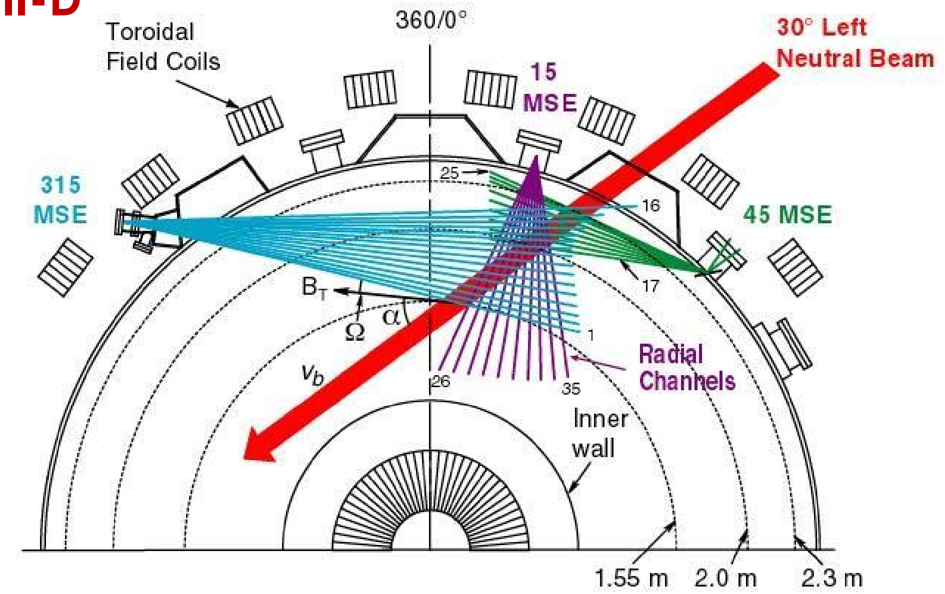

Integrated modelling for current components

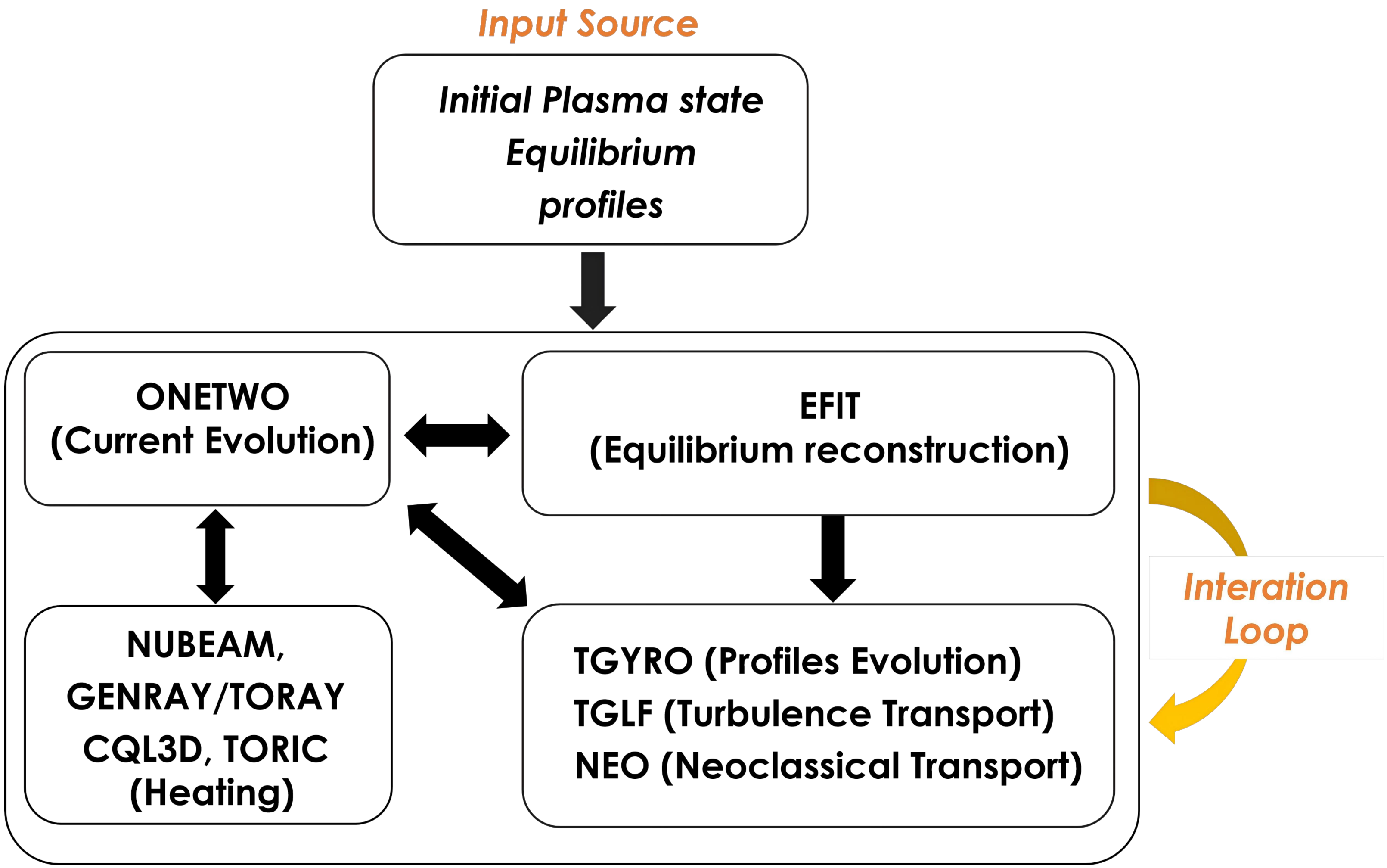

Using OMFIT for integrated modeling determine current component.

- **Prescribe:density/rotation/ pedestal profiles**
- **Couple H-CD-transport-equilibrium**
- **Modules:**
  - **TGYRO: evolve Te/Ti**
  - **ONETWO: evolve current,sources and sinks**
  - **EFIT: G-S solver**

Integrated modelling for current components

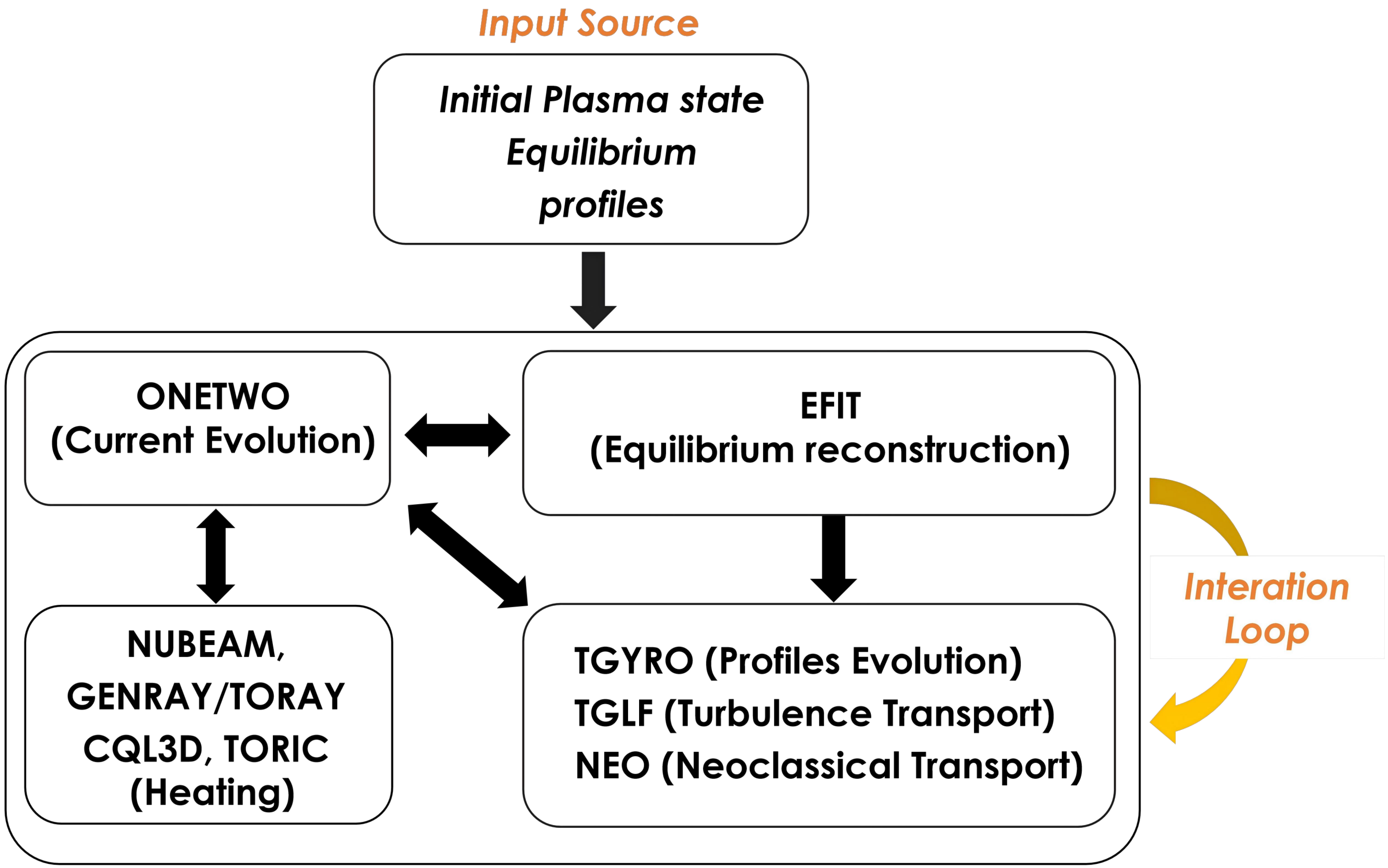

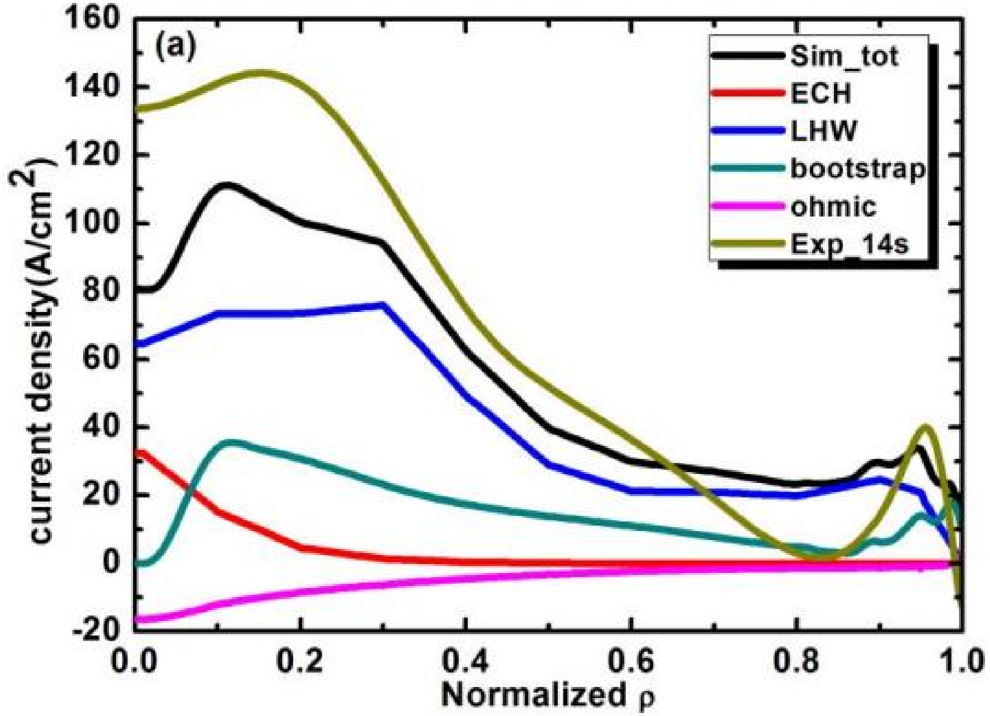

Wu et al, 2018 NF 58 046001

Dignostics/indicators for H & CD

Parameters	Diagnostics/indicators
Te	TS, ECE
Ti	CXRS, XICS
W_{dia}	Diamagnetic loop coils
Inductive current	loop voltage
J, q	MSE/Polarimeter + equilibrium reconstruction
Neutron rate	Neutron camera, NFM
Radiated power	Soft-X ray, Bolometer
Fast particle distribution	FIDA, NPA
H&CD deposition	MHD activities (NTM, ST period, AE,...)

Deposition of H & CD is essential

Deposition location and width are as critical as total power, as for ECCD, ICRH mode conversion, NBI fast-ion deposition.

Methods:

- ☐ Ray-tracing simulation
- ☐ Break-in-slope analysis
- ☐ Heat pulse propagation
- ☐ MHD marker (alignment scan)

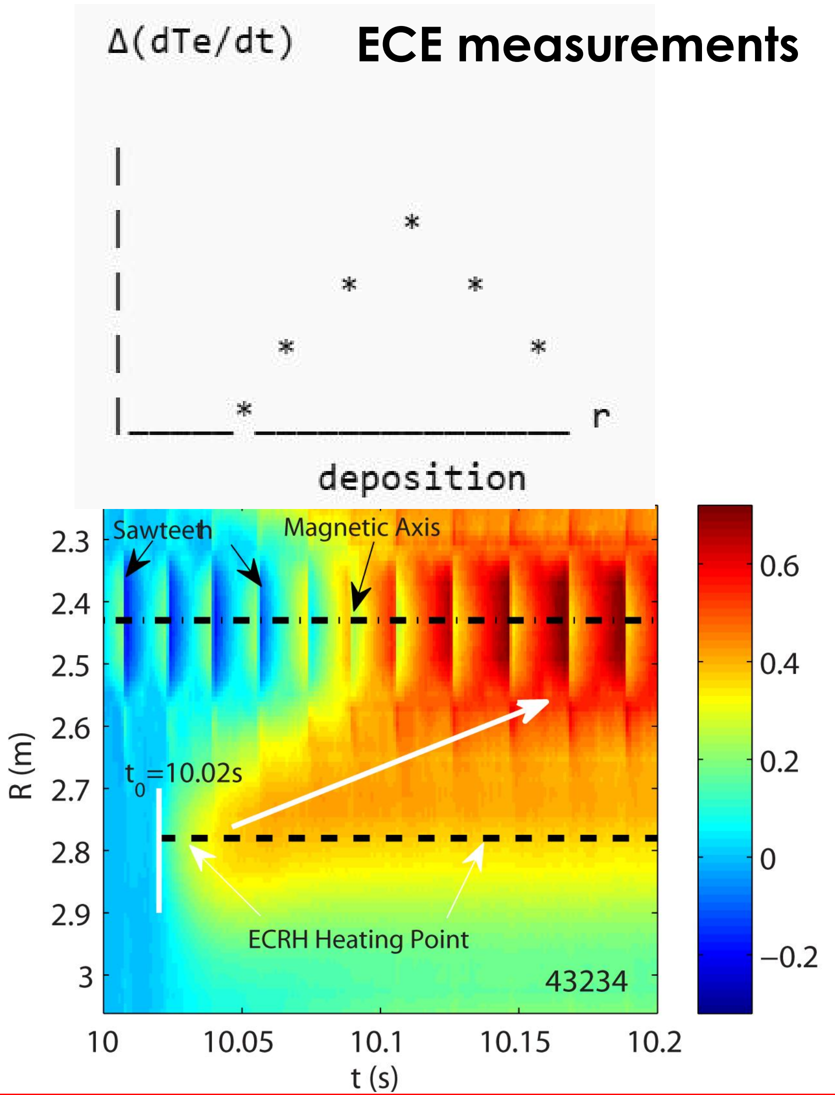

Deposition of H & CD is essential

Deposition location and width are as critical as total power, as for ECCD, ICRH mode conversion, NBI fast-ion deposition.

Methods:

- ☐ Ray-tracing simulation
- ☐ Break-in-slope analysis
- ☐ Heat pulse propagation
- ☐ MHD marker (alignment scan)

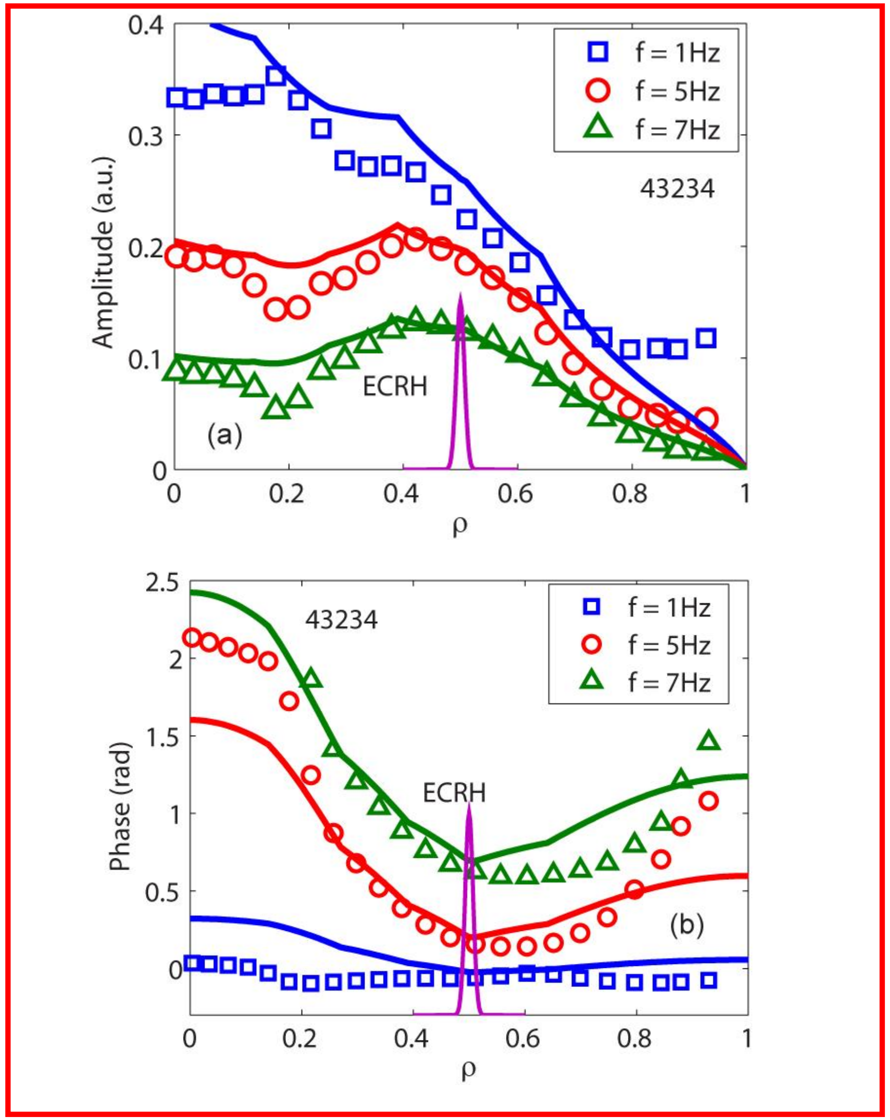

Fourier transform: peak in amplitude and trough in phase are consistent with deposition by Ray tracing.

Song Shaodong, PHD thesis

Outline

- Physical requirements for H&CD
- Overview of H&CD systems from experimental perspective
- Measurements of H&CD
- **Application in fusion experiments**
  - **Profiles control and transport study**
  - H-mode access
  - Fast-ion physics
  - Integrated control and scenario optimization
- Summary

JT-60U: 45 keV Ti obtained in High β_p H-mode

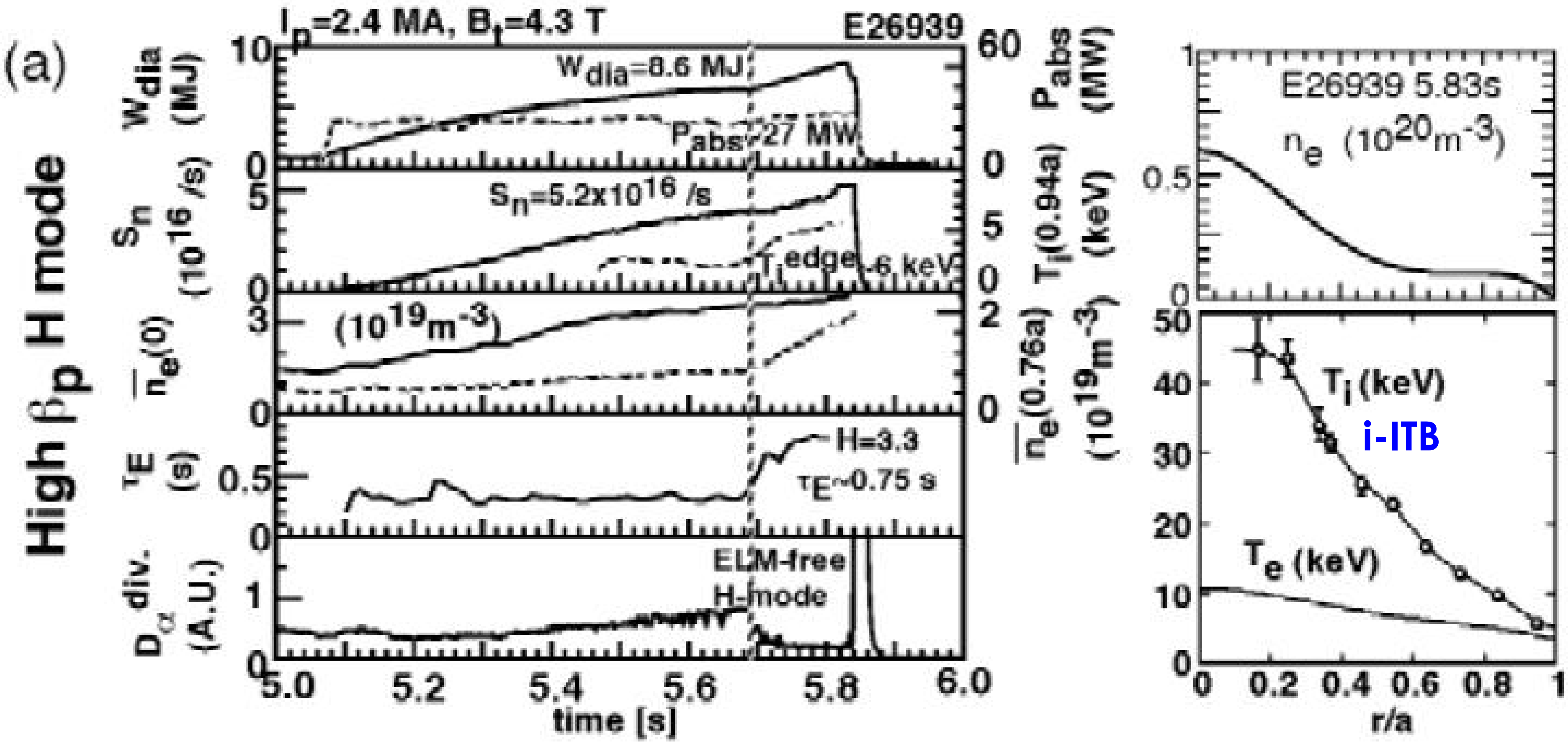

Ip=2.4 MA, Bt=4.3 T, q_{95}=2.9, P_{abs}=27 MW, RS plasma

$\mathbf{n_D(0)\tau_E T_i(0) = 1.5 \times 10^{21} m^{-3} \cdot s \cdot keV}$, **$T_i(0)$=45 keV**, $\boldsymbol{\beta_p = 1.15}$, $\boldsymbol{\beta_N = 2.0}$, $\boldsymbol{H_{89p}}$**=3.3**

Y. Kamada, Fusion Science and Technology, 42 185-254 (2002)

HL-3: High triple product in NBI-heated plasma

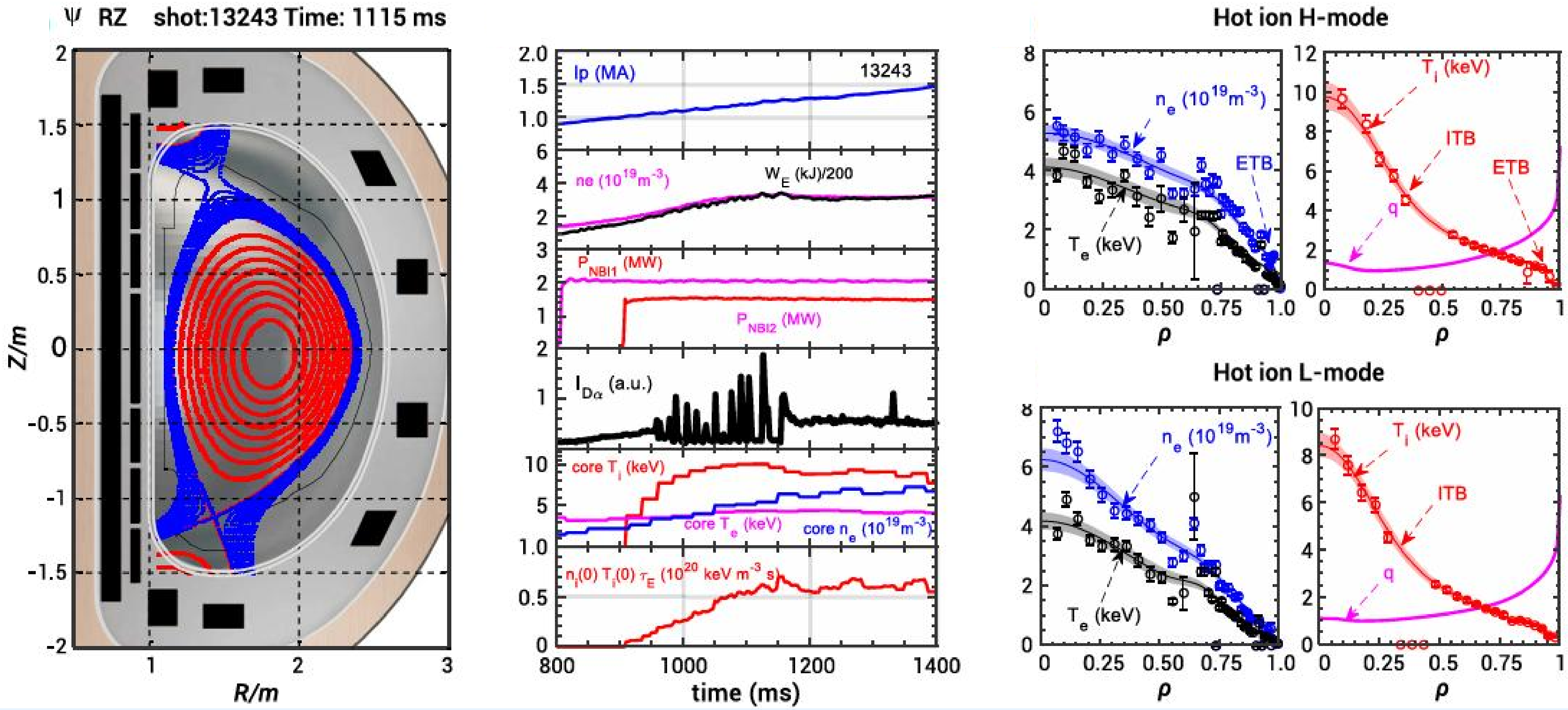

1-1.5 MA, P_{NBI}=3.5 MW, T_i~10.1 keV, DTB, $n_e\tau_E T_i \sim 0.7 \times 10^{20}\ keV \cdot m^{-3} \cdot s$

Zhong W., The Innovation 7(2), 101167 (2026).

EAST: 1066s H-mode with ECCD and LHCD

Bt~2.5T/LSN, H_{98y2}~1.35, n_e/n_G ~0.6, f_{BS} ~50%, T_{e0}~10keV, E_{inj}~3.05GJ

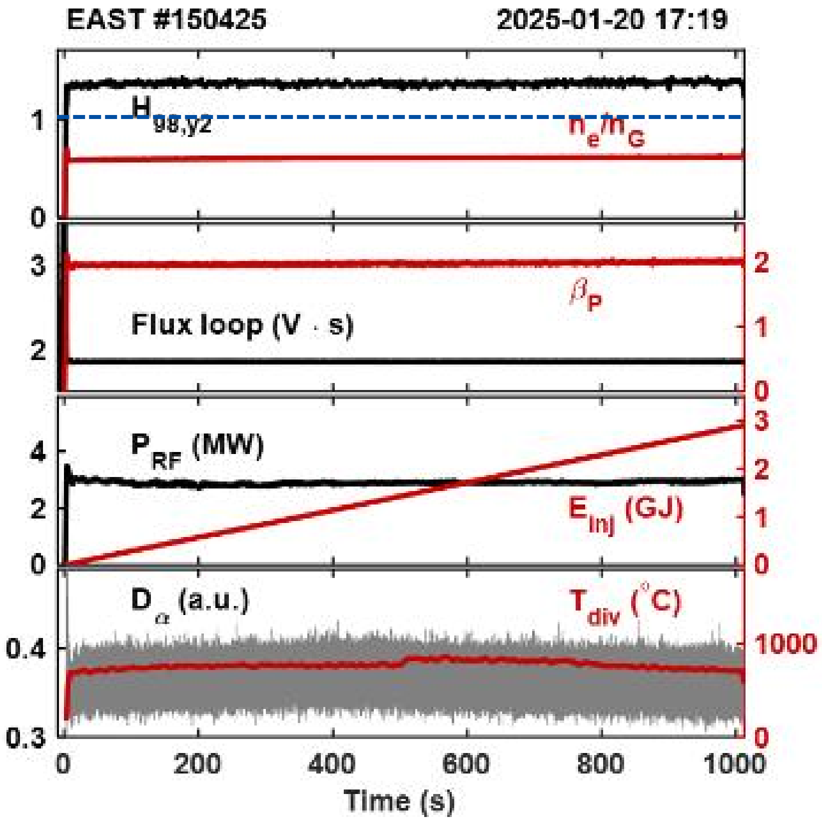

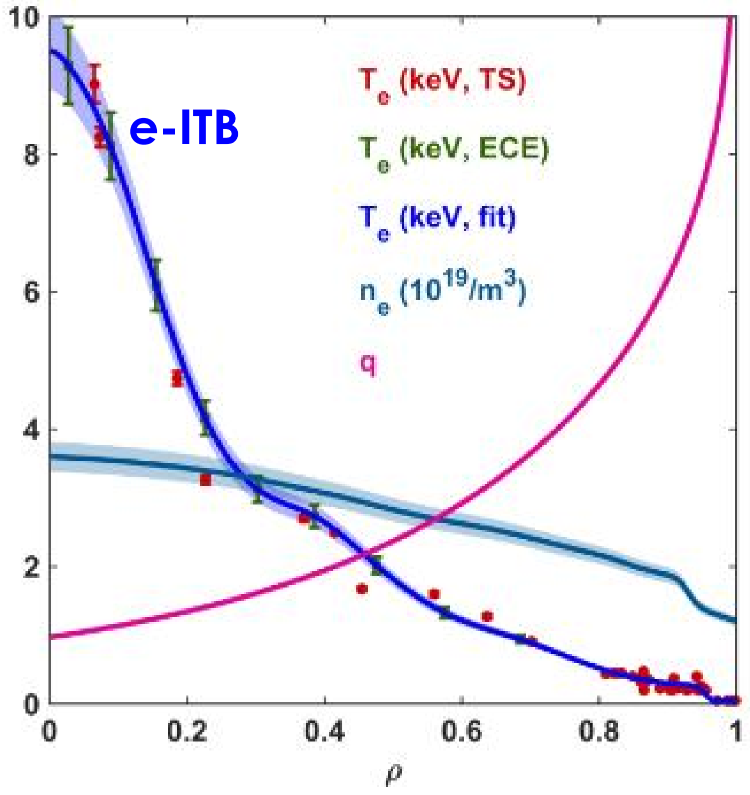

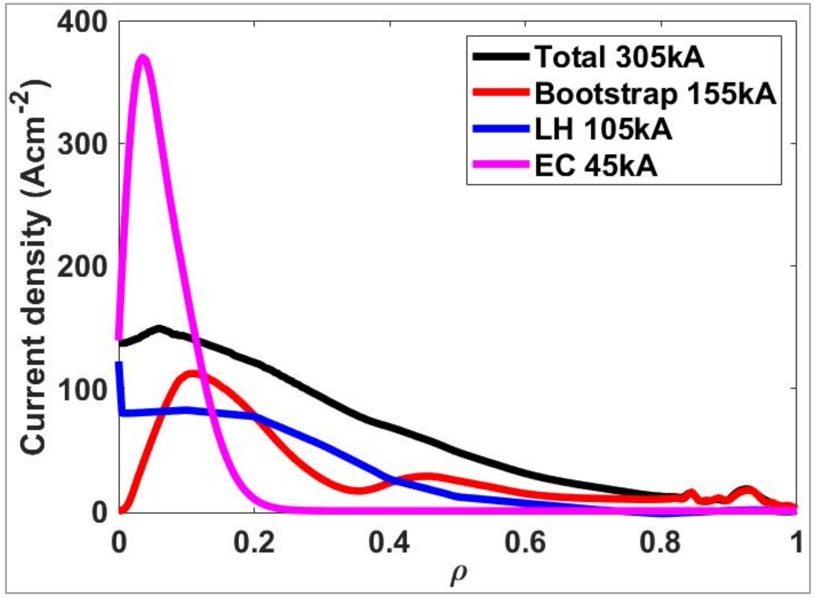

X. Gong, 30th IAEA FEC (2025)

C-Mod: Fully non-inductive CD by LHCD

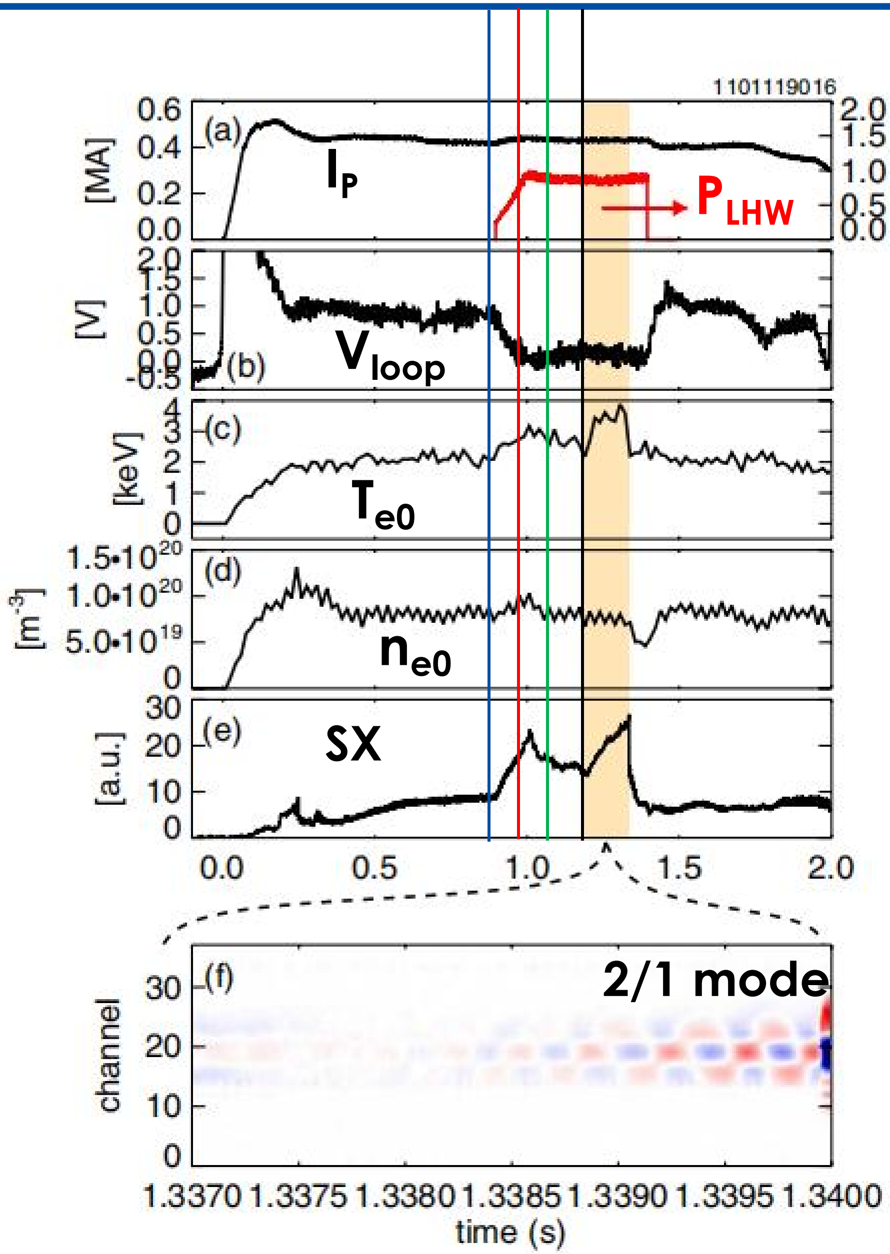

S. Shiraiwa et al 2013 NF 53 113028

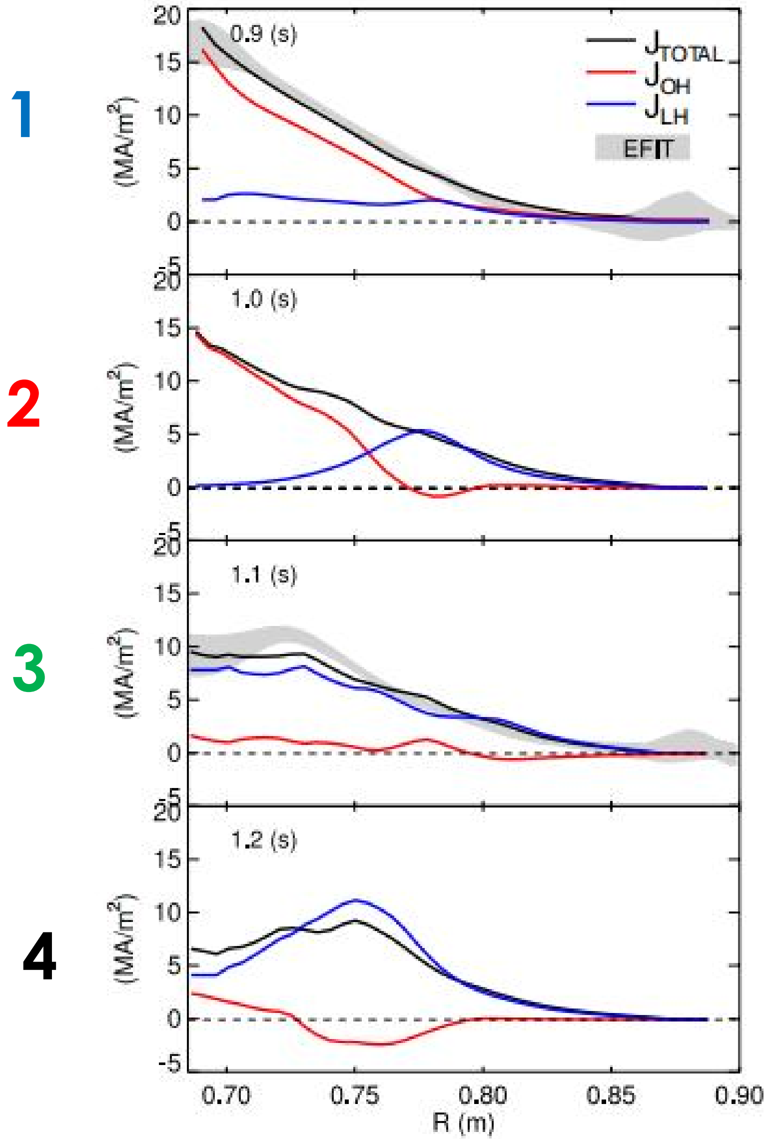

Before LHW, OH dominated.

1 MW LHW, off-axis CD.

Fully non-inductive CD with loop voltage ~ 0

Off-axis J_{total}
RS → e-ITB onset

JT-60U: Te-, ne-, Ti-ITBs formation in RS plasmas

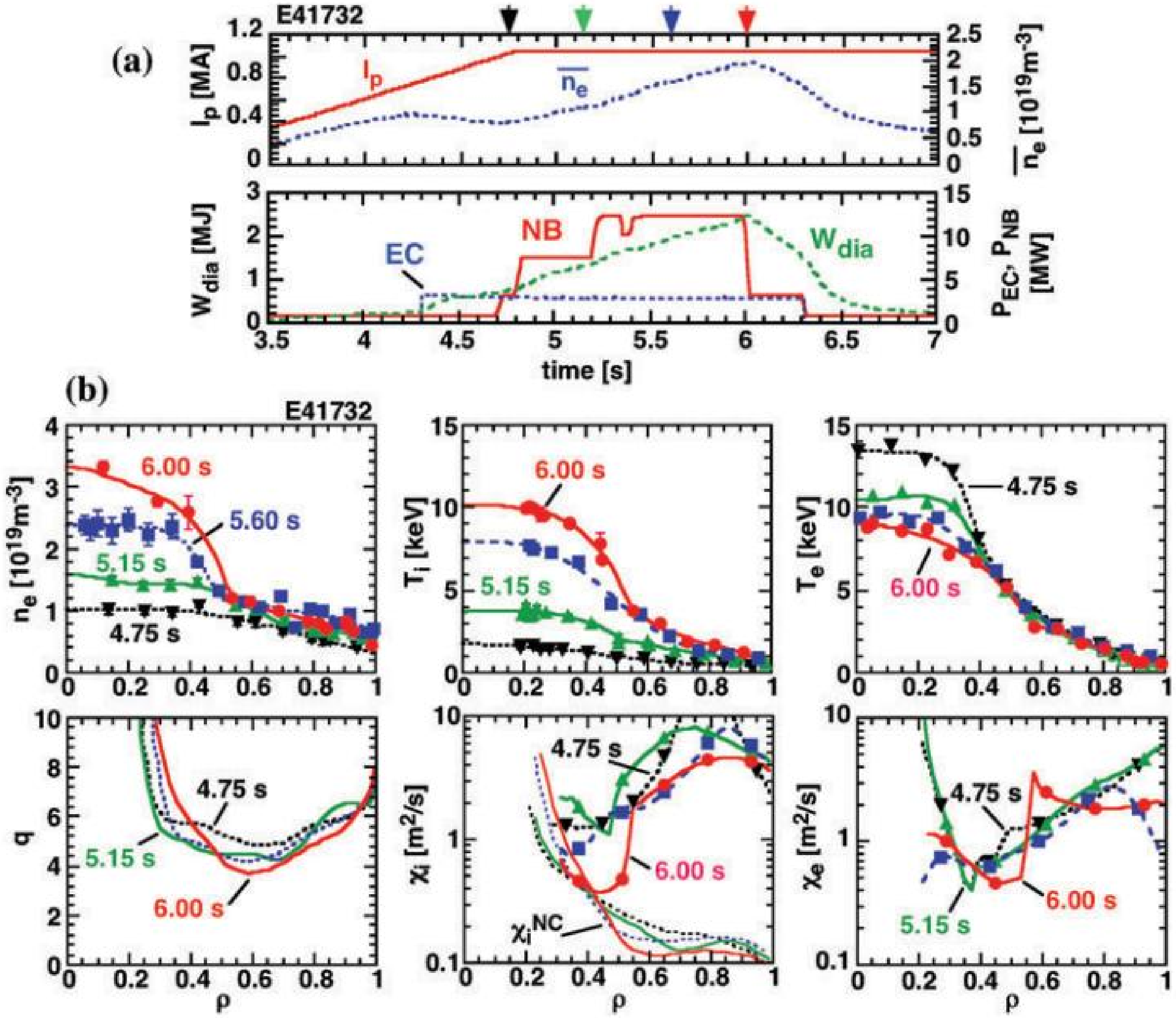

T Fujita et al 2004 PPCF 46 A35

- ☐ 4.75s: strong e-ITB by EC heating
- ☐ 5.15s: ne and Ti-ITB onset, and Te-ITB sustains
- ☐ 5.6 s: clear ne, Ti, Te-ITBs
- ☐ ITB foot were similar for both Te and Ti indicating a strong linkage between electron and ion ITBs.
- ☐ χi decreased with increase in NB power (due to Er gradient)
- ☐ Electron thermal diffusivity χe remained almost constant (main factor is the magnetic shear).

Power balance analysis

Energy conservation $P_{\text{in}} = P_{\text{loss}} + \frac{dW}{dt}$

$$\frac{\partial W_e}{\partial t} = P_e - \nabla \cdot Q_e - P_{ei}$$

$$\frac{\partial W_i}{\partial t} = P_i - \nabla \cdot Q_i + P_{ei}$$

$W_{e,i} = \frac{3}{2} n T_{e,i}$ stored energy

$P_{e,i}$: absorbed power

$Q_{e,i}$: heat flux

P_{ei}: collisional exchange power between electron and ion

For SS, $Q_e(r) = \frac{1}{A(r)} \int_0^r P_e(r') dV$, A is area unit, V is volume unit

Measured ne,Te,Ti, ∇Te, ∇Ti

from Modelling

Local diffusive model, $\chi_e = -\frac{Q_e}{n_e \nabla T_e}$ ⟶ effective χ_e

TRANSP/OMFIT/JINTRAC/ASTRA integrate all heating sources, profile data, and power-balance equations to calculate heat fluxes and transport coefficients.

Perturbative transport study

Modulation experiments + Fourier transform

Heating schemes	Parameters	Transport coefficient
NBI	ne, Ti, V_{ϕ}	D, V, χ_i. χ_{ϕ}
ECRH	T_e	χ_e
ICRH	ne, Ti, Te	D, V, χ_i. χ_{ϕ}
LHCD	Te	χ_e

LHD: ECRH modulation for heat transport

S. Inagaki, NF 53 (2013) 113006

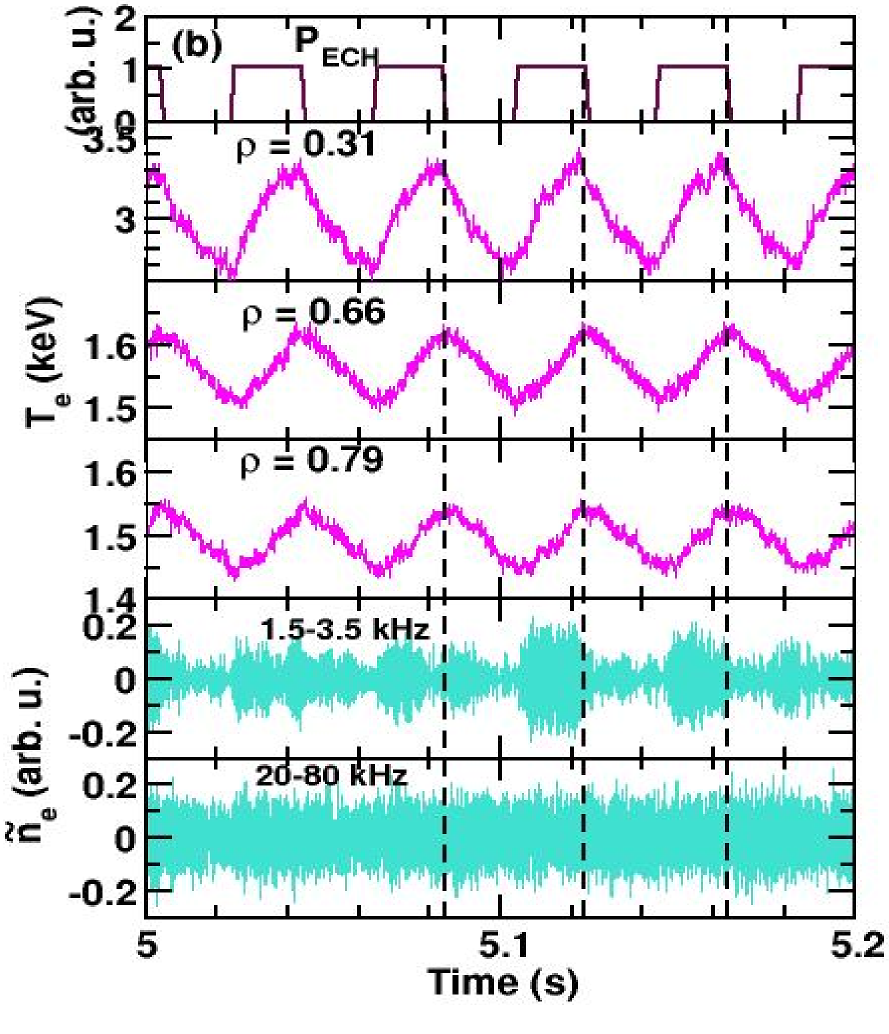

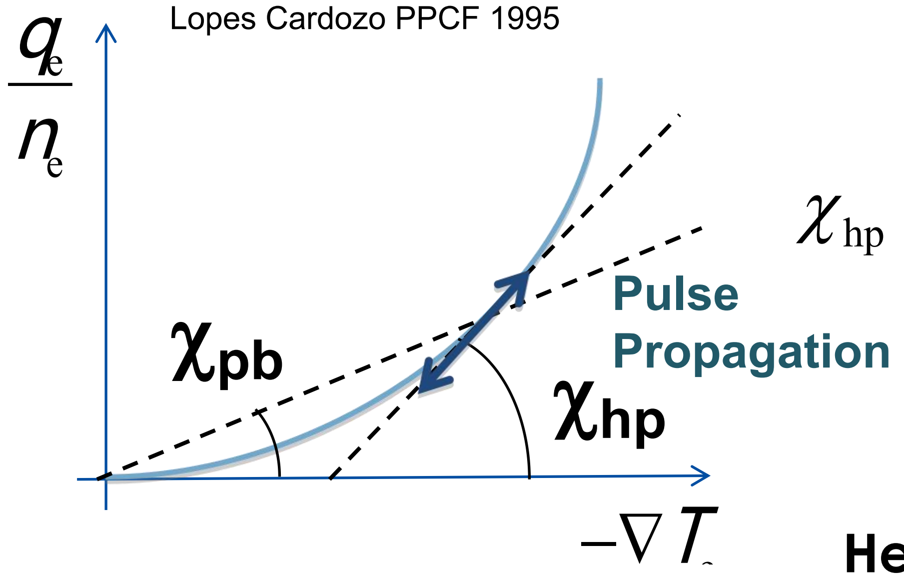

$$\chi_{hp} = \frac{-\partial q_e}{n_e \partial \nabla T_e} \neq \frac{-q_e}{n_e \nabla T_e} = \chi_{pb}$$

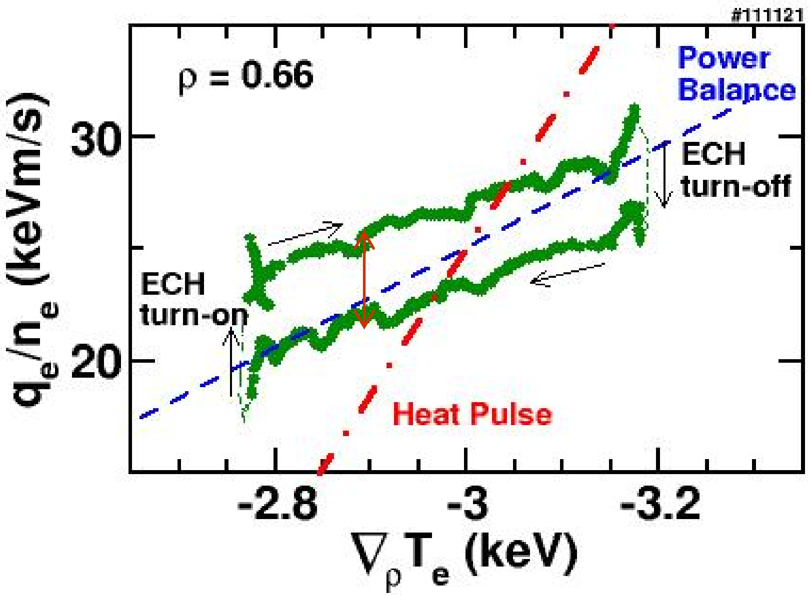

Heat flux q_e:

- ☐ **A jump between ECH-on and -off;**
- ☐ **Smooth change in q_e associated with change in ∇T_e**

Fick's law violation: change in qe has hysteresis effect.

Tore Supra: ICRH modulation for particle transport

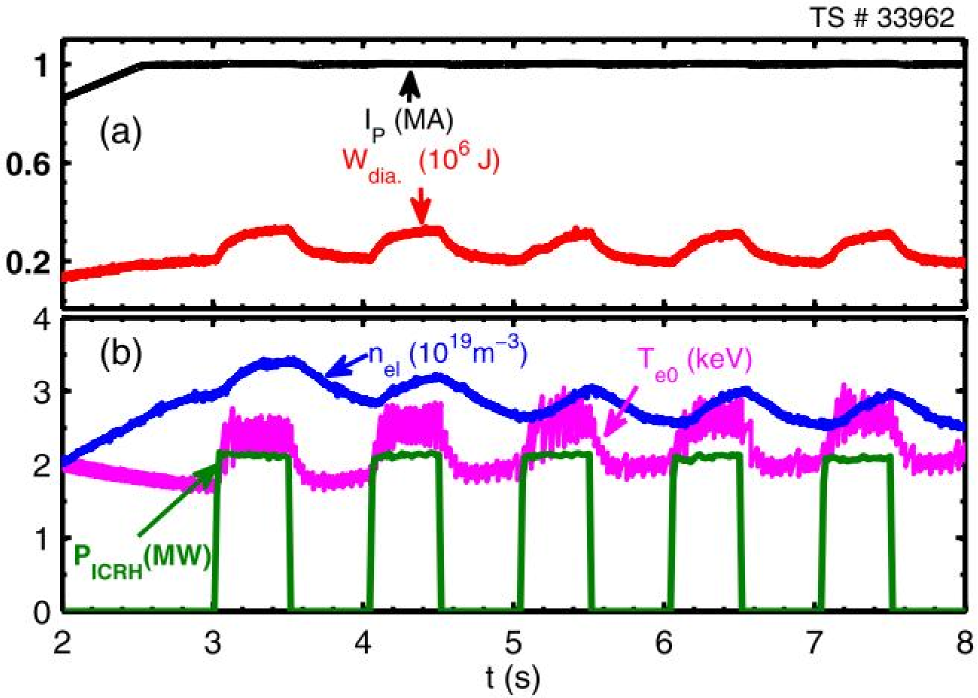

W. L. Zhong, PRL 111, 265001 (2013)

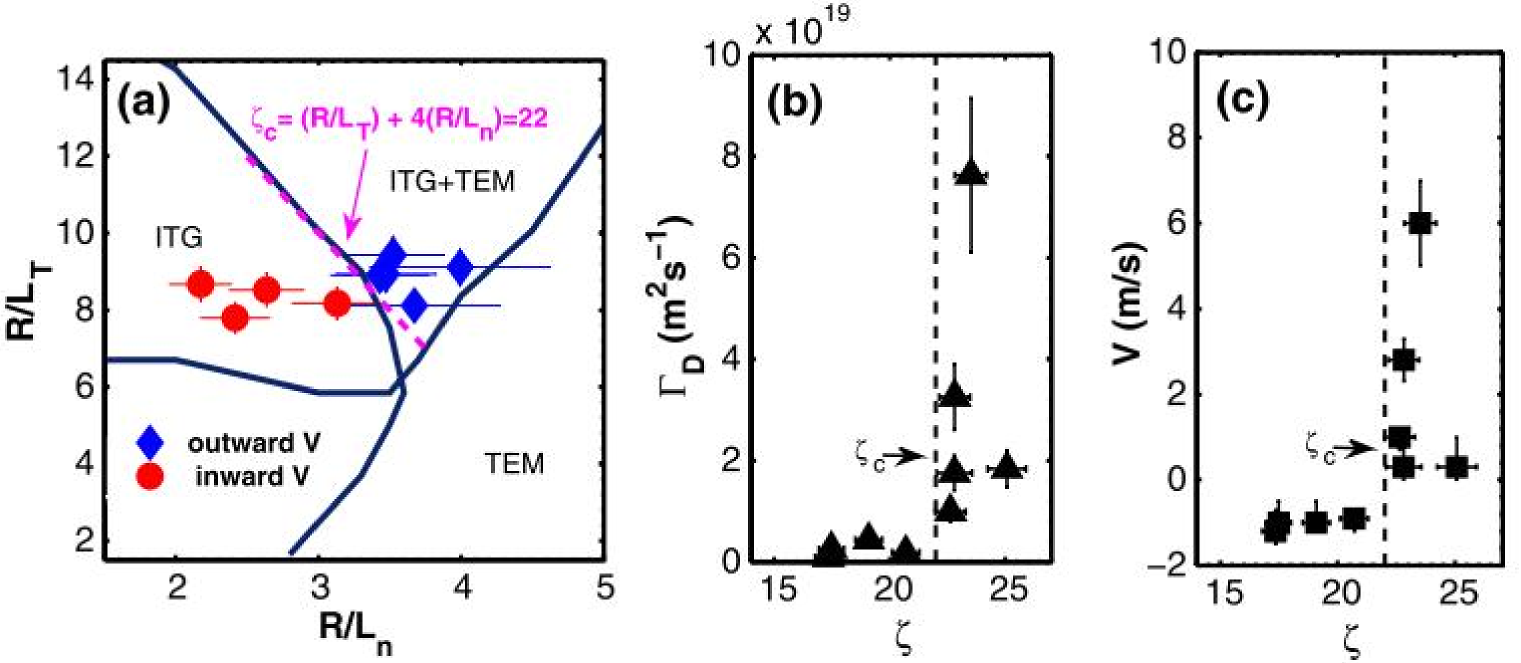

ξ=R/L_T +4(R/L_n)

- **ICRH modulation→ ne and Te gradient changes**
- **Reversal of the particle convective velocity and a strong increase in the turbulent particle flux when exceeding a mixed critical gradient R/L_T +4(R/L_n)= 22**
- **Transition from ITG to ITG+TEM turbulence**

Rotation: Momentum transport

$$\Pi_\phi = -\chi_\phi \nabla V_\phi + V_\phi^{pinch} V_\phi + \Pi_{\text{res}}$$

↑ **NBI torque**

↑ **driven by turbulence**

↑ **RF heating**

Turbulence transports momentum through diffusion, convection or a pinch, and a residual-stress term.

LHD: Rotation changed by NBI injected geometry

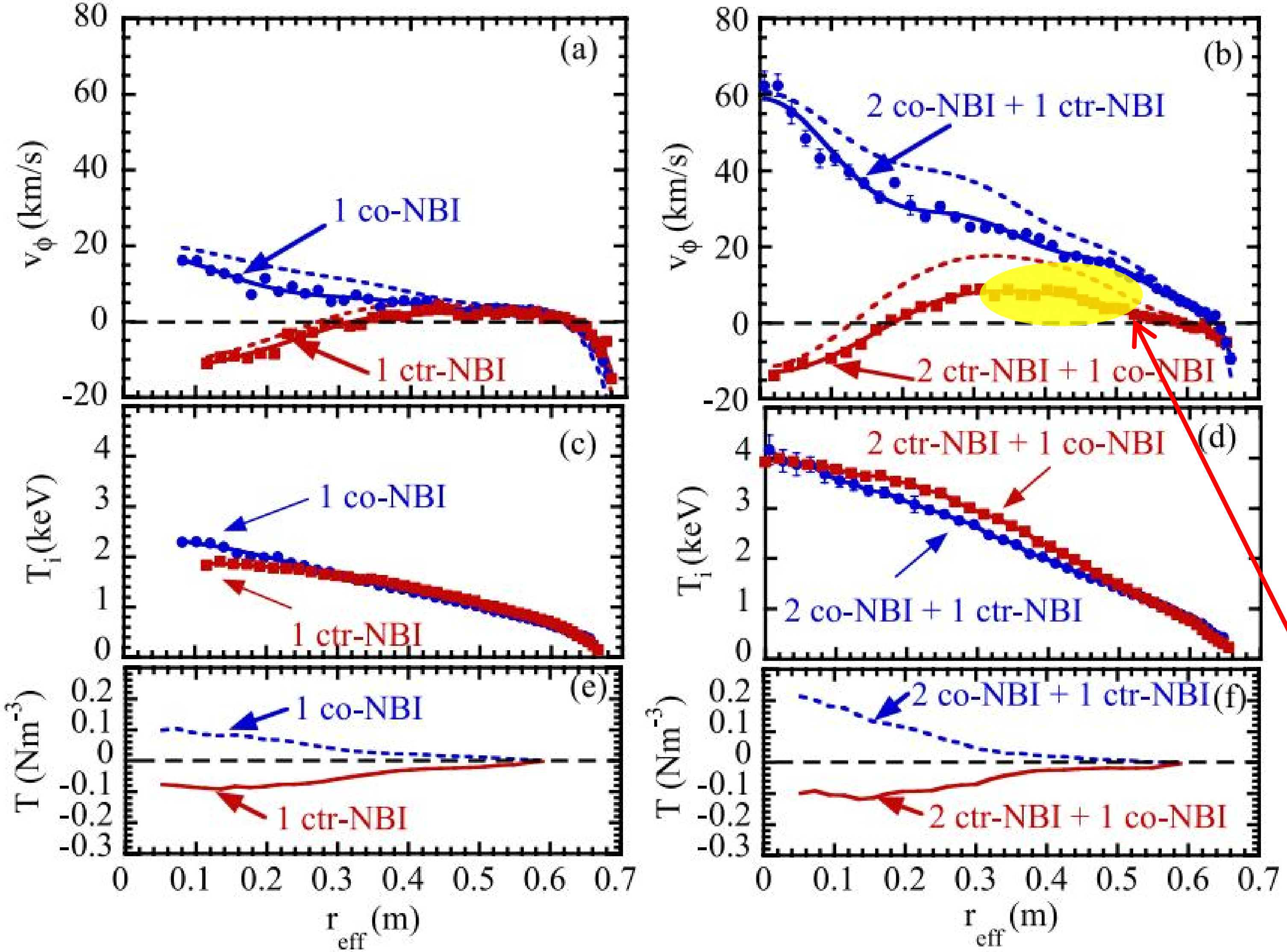

K. Ida, 2010 NF 50 064007

(a): Rotation profile of 1co-NBI is similar to 1 ctr-NBI except for the sign differences.

(e) and (f): net toroidal torques are somewhat similar

(b): Three NBIs: V_ϕ profile with ctr-NBI dominant discharge is quite different from co-NBI dominant discharge

Spontaneous rotation in the co-current direction due to large ∇P_i after ITB formation

JT-60U: Intrinsic rotation driven by ECRH

Balanced NBI, P_{NBI}=4.9 MW

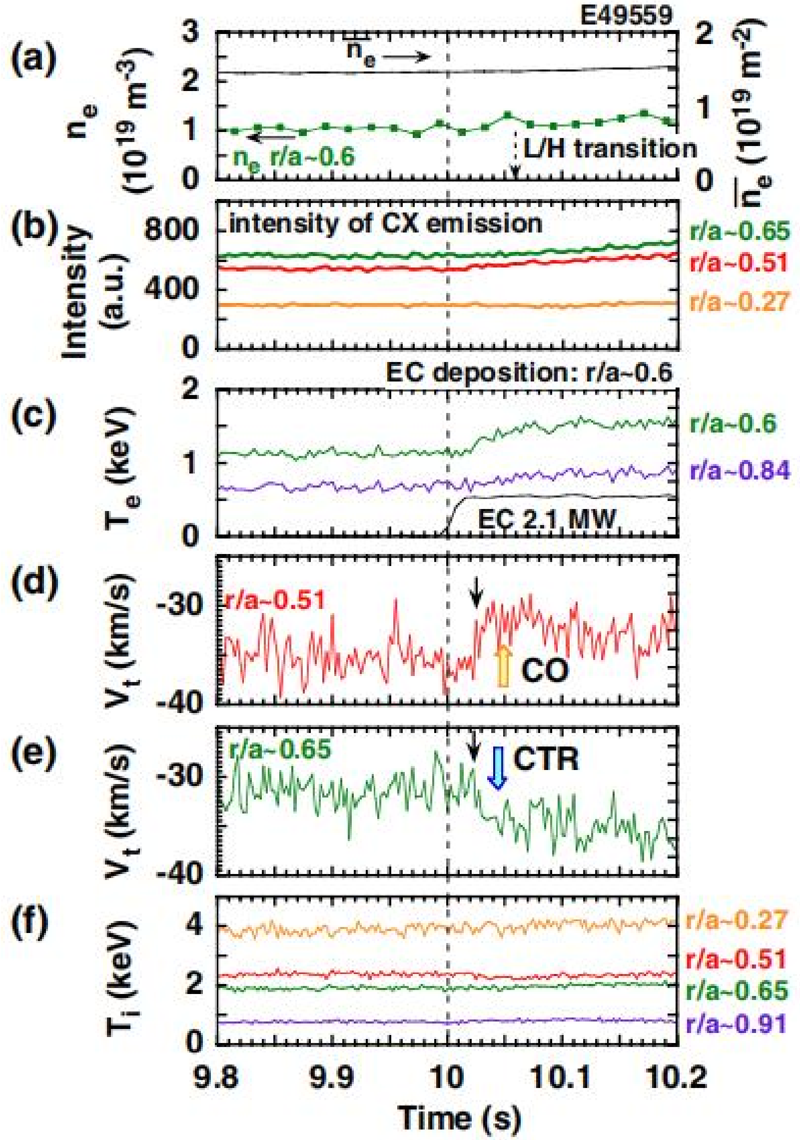

Yoshida M. et al 2009 PRL 103 065003

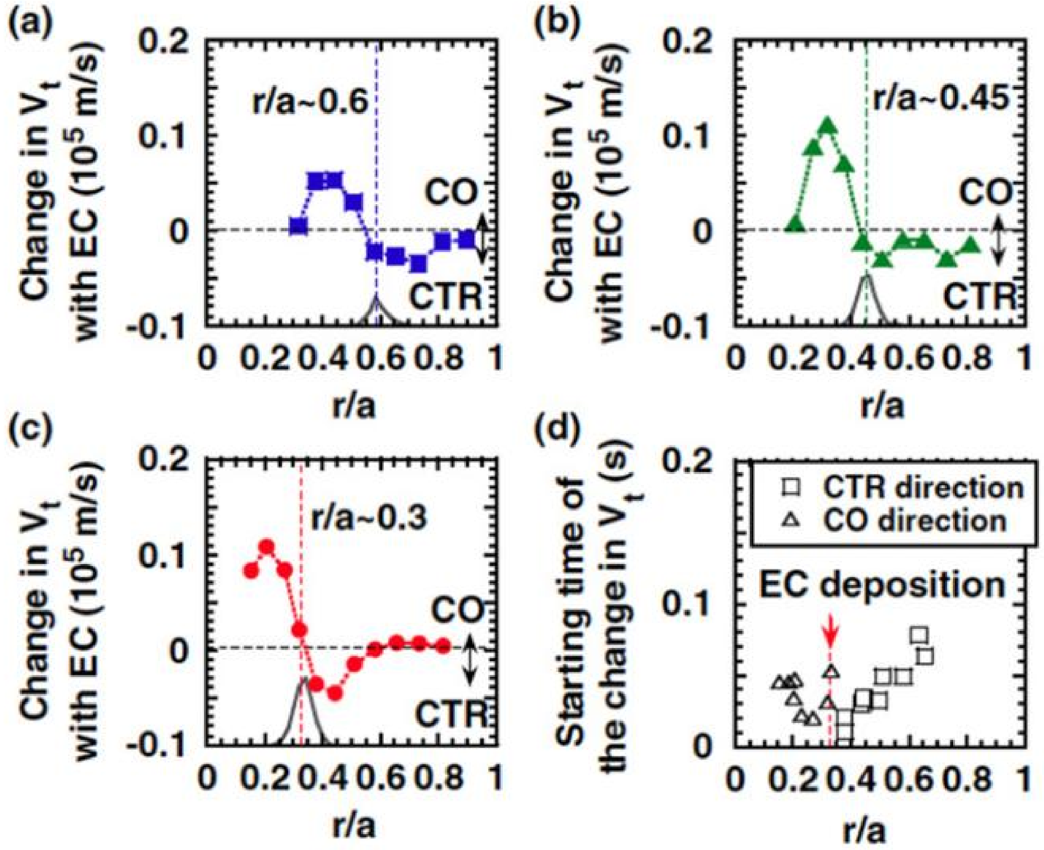

- ECH drives co-(counter-) intrinsic rotation inside (outside) of the EC deposition radius.
- Possibilities: turbulence driven intrinsic torque, more negative Er

C-Mod: Toroidal rotation driven by ICRF mode conversion

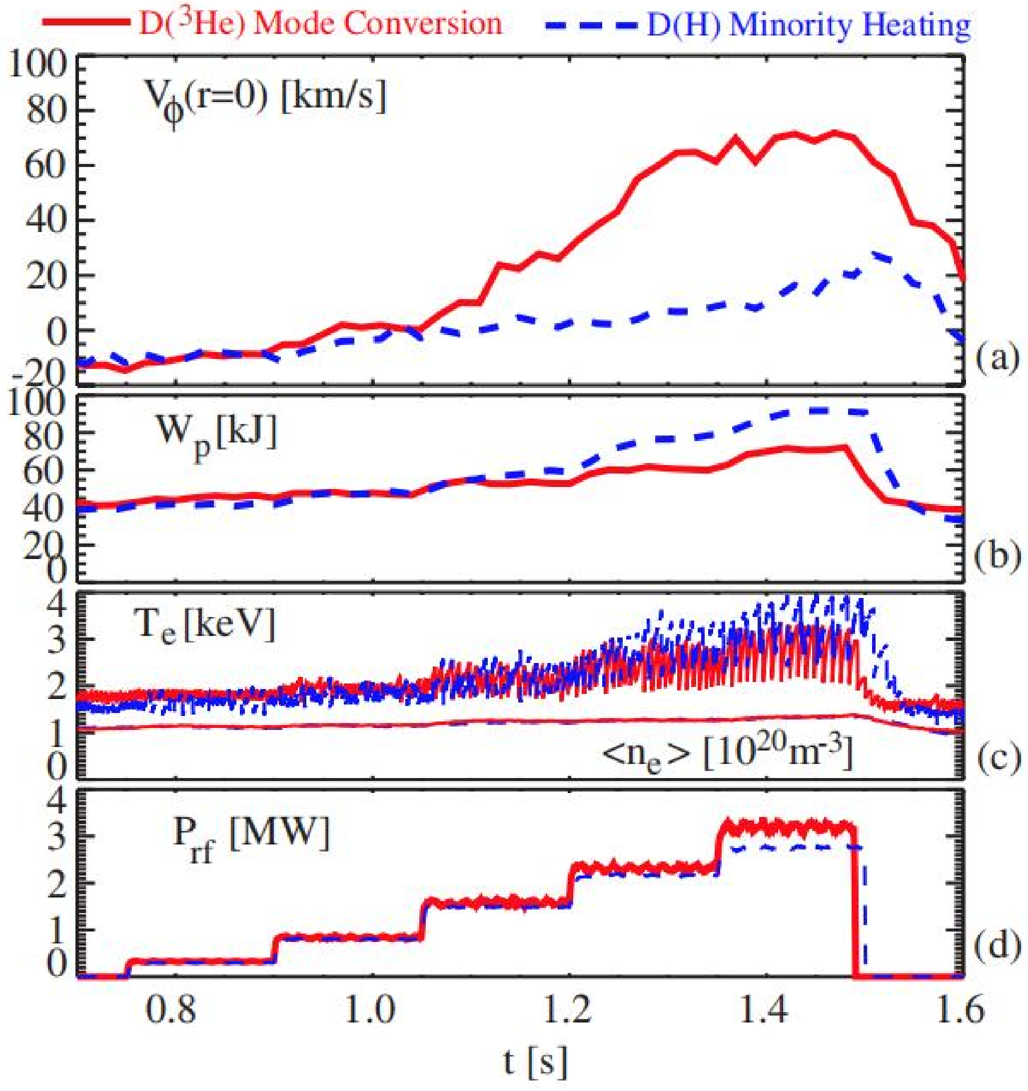

Lin Y. et al 2008 PRL 101 235002.

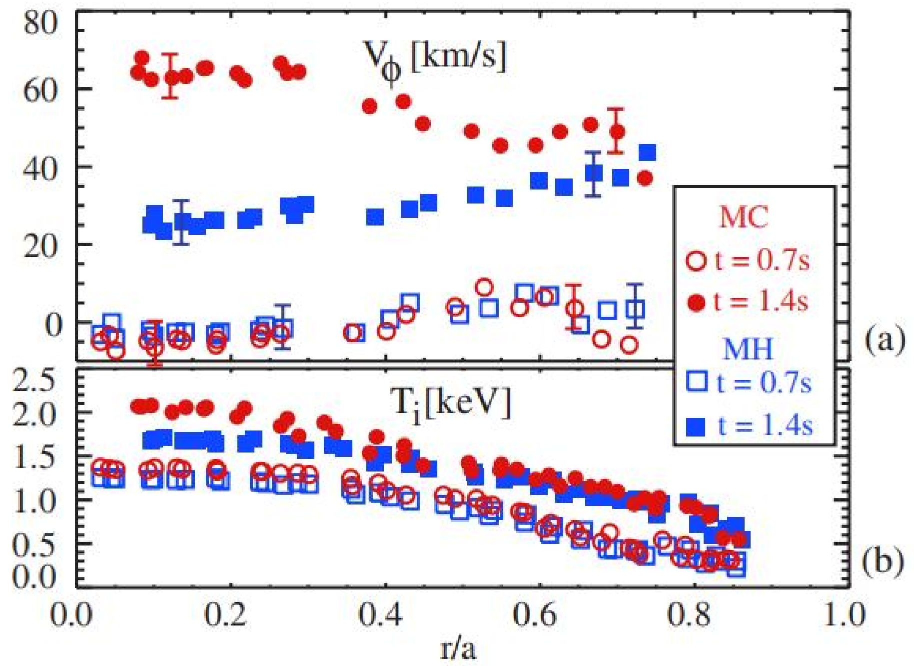

- ◻ V_ϕ is significantly higher (-10→75km/s) in the MC plasma than MH plasma (-10→ 20km/s).
- ◻ ΔV_ϕ is approximately linear vs P_{ICRF}, indicating RF power dissipation is important, rather than direct momentum transfer from RF EM field itself.

HL-2A: Impurity transport enhanced by ECRH

Z.Y. Cui, NF 58 056012 (2018)

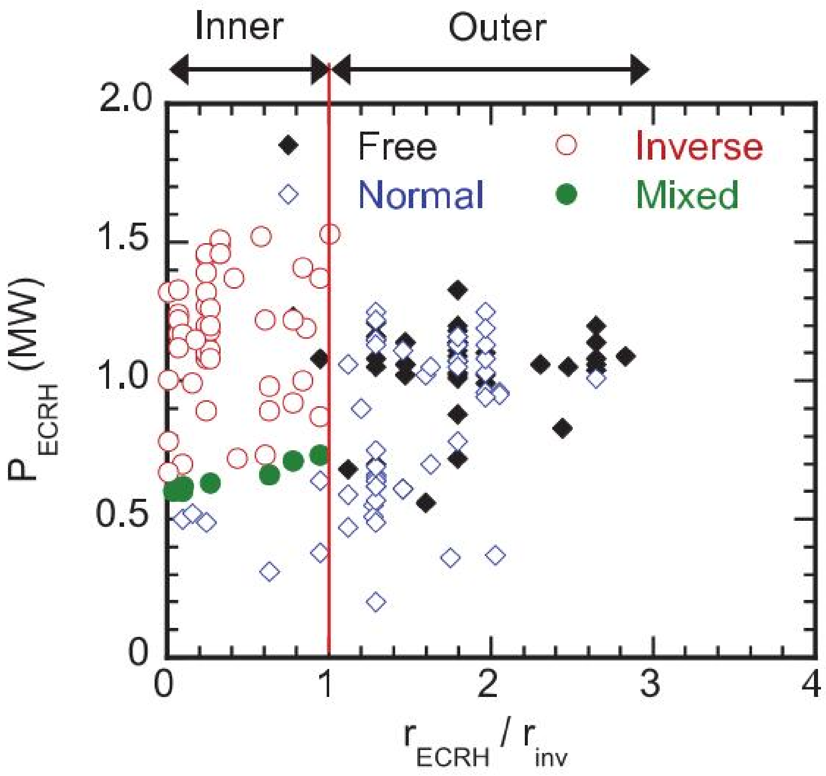

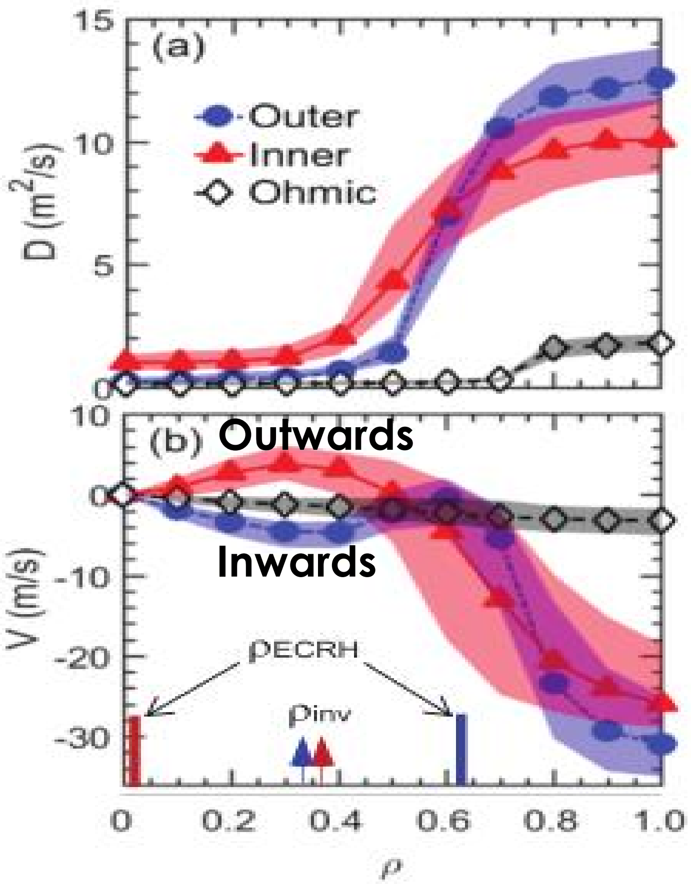

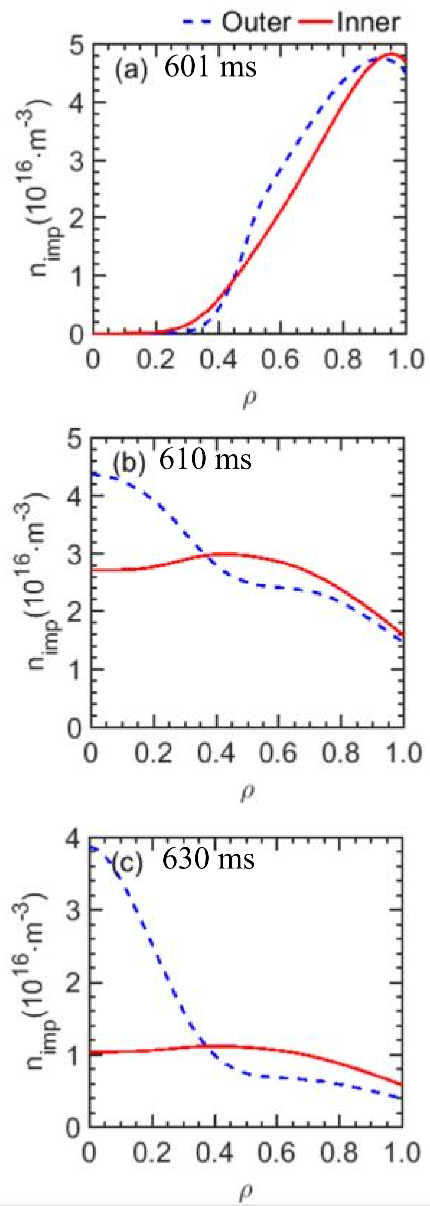

Inner-deposited (inside ST inversion radius) ERCH:

- ☐ **Inverse sawtooth oscillation observed**
- ☐ **Outward convective velocity of Al impurity develops**
- ☐ **Al ion density profile flattened.**

Outline

- Physical requirements for H&CD
- Overview of H&CD systems from experimental perspective
- Measurements of H&CD
- **Application in fusion experiments**
  - Profiles control and transport study
  - **H-mode access**
  - Fast-ion physics
  - Integrated control and scenario optimization
- Summary

Energy confinement time scaling

L-mode:

$$\tau_E \text{ (ITER89-P)} = 0.048\, M^{0.5}\, I^{0.85}\, n^{0.1}\, B^{0.2}\, \kappa^{0.5}\, R^{1.2}\, a^{0.3}\, P^{-0.5}$$

ELMy H-mode:

$$\tau_E \text{(IPB98(y,2))} = 0.145\, M^{0.19}\, I^{0.93}\, n^{0.41}\, B^{0.15}\, \kappa^{0.78}\, R^{1.39}\, a^{0.58}\, P^{-0.69}$$

$$H\,factor = \frac{\tau_E}{\tau_{E(\text{L-mode})}} \rightarrow \frac{\tau_E}{\tau_{E(\text{IPB98, y2})}}$$

H-mode access and P_{LH} scaling

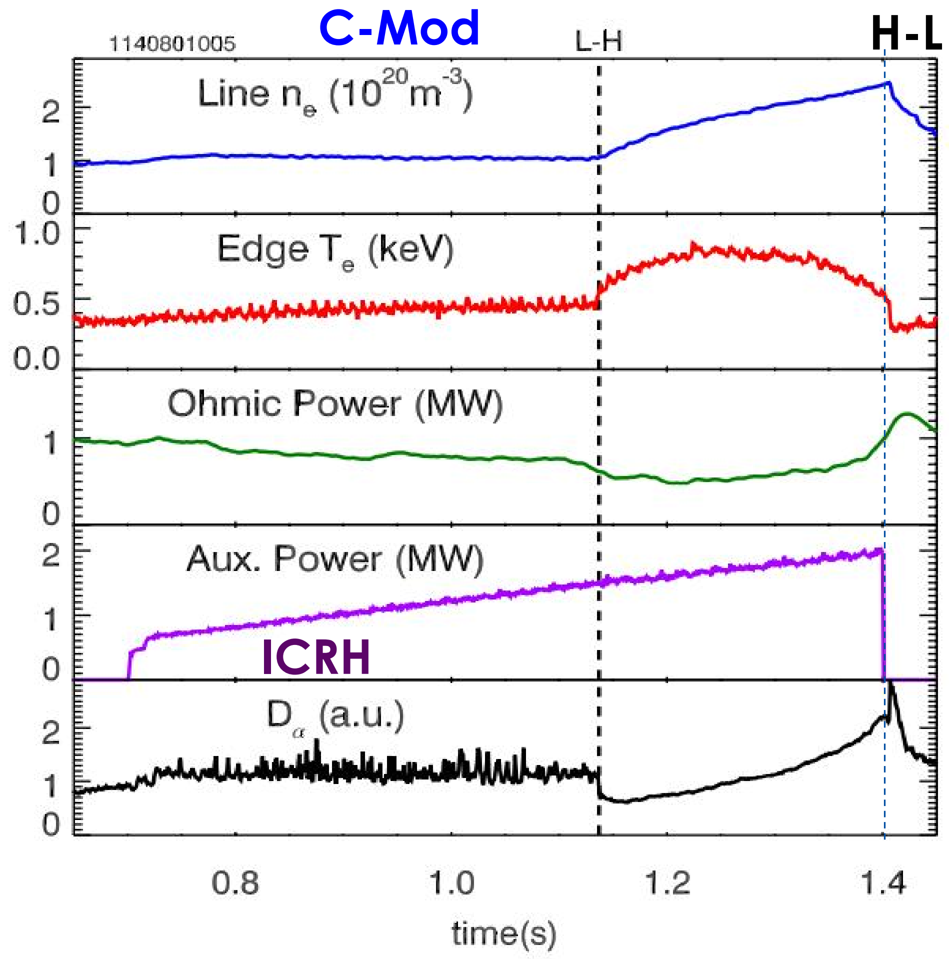

H-mode access when heating power exceeds a threshold, P_{LH}

M. Schmidtmayr, NF 58 (2018) 056003

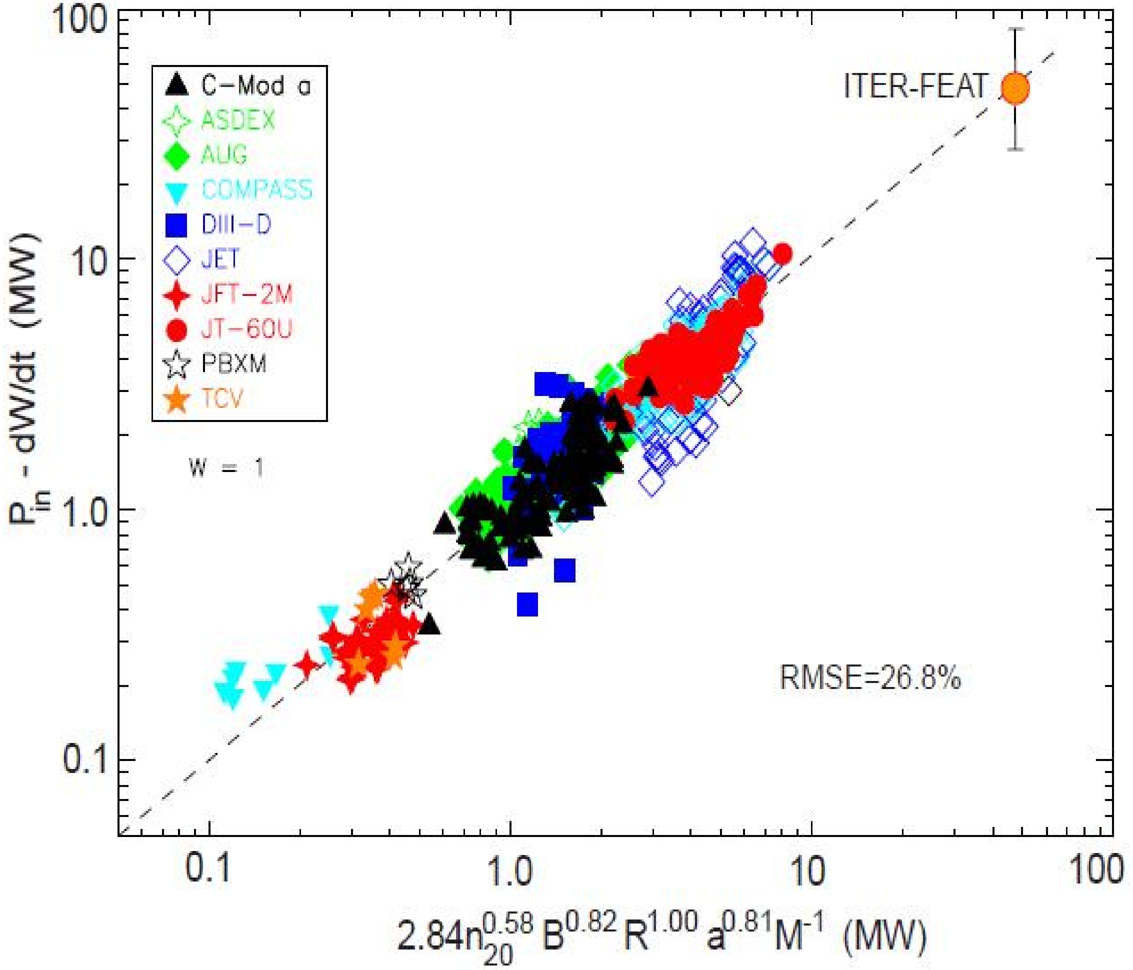

Type I-ELMy H-mode:

$$P_{LH}^{98(1)} = 2.84\bar{n}_{20}^{0.58} B^{0.82} R^{1.00} a^{0.81} M^{-1}$$

Effect of heating on P_{LH}

AUG: F. Ryter, 2014 NF 54 083003

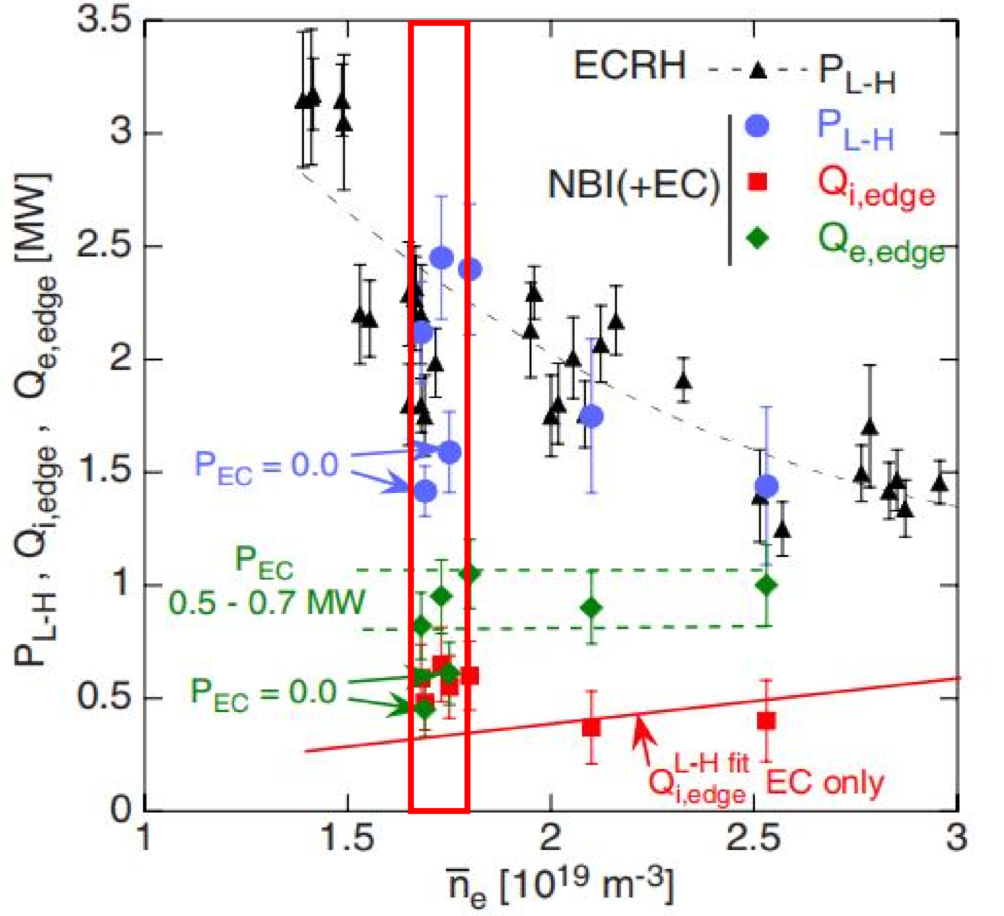

- **With NBI alone, P_{LH} ~40% lower than ECRH points → importance of ion heating in LH transition**
- **Added ECRH power NOT contribute to ion heat flux (L–H transition trigger)**

Outline

- ☐ Physical requirements for H&CD
- ☐ Overview of H&CD systems from experimental perspective
- ☐ Measurements of H&CD
- ☐ **Application in fusion experiments**
  - ➢ Profiles control and transport study
  - ➢ H-mode access
  - ➢ **Fast-ion physics**
  - ➢ Integrated control and scenario optimization
- ☐ Summary

DIII-D: Multiple AEs driven in NBI heated RS plasmas

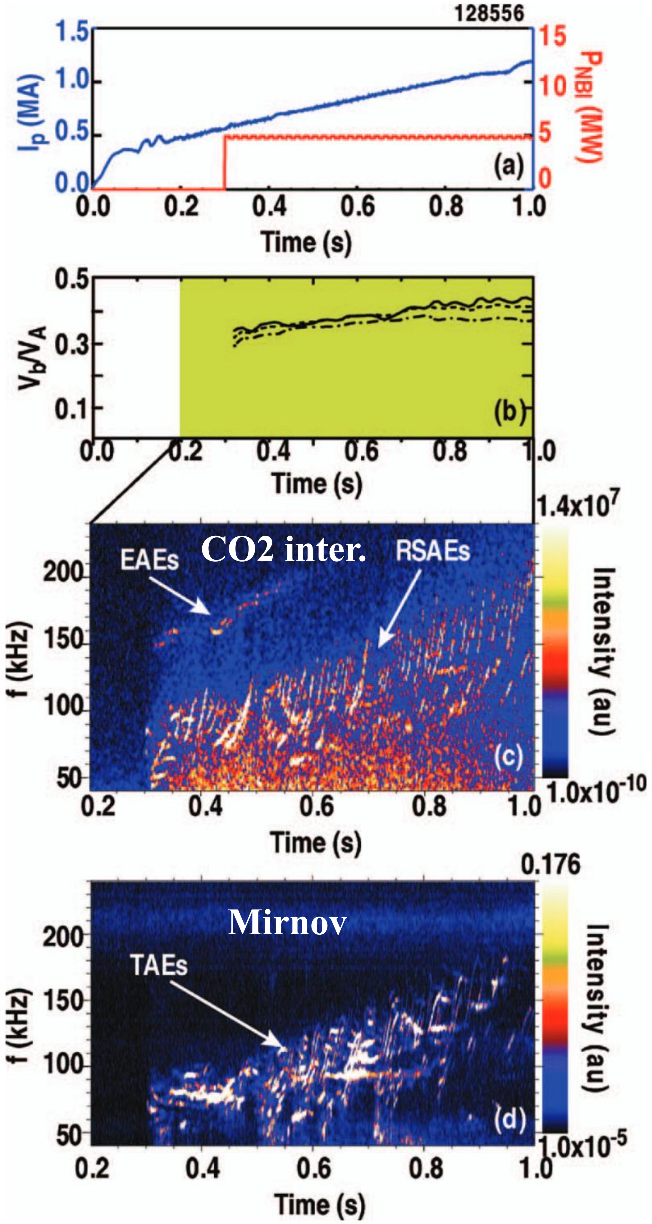

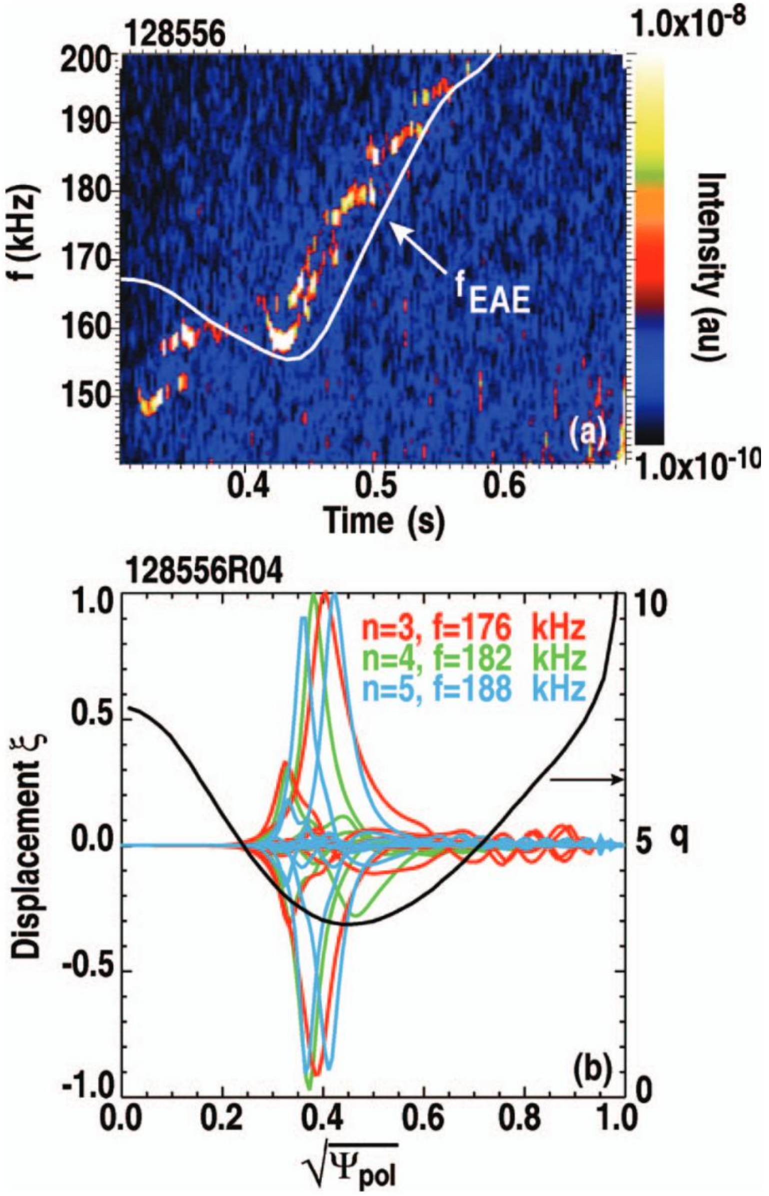

- ☐ TAEs, RSAEs and EAEs driven by fast ions observed during NBI in RS plasmas.
- ☐ EAEs require higher fast ion velocities, twice of TAE frequency
- ☐ Beam ions transfer energy to the AEs via high-order resonances, which redistributes or expels fast ions.

R.Nazikian 2008 Phys. Plasmas 15, 056107

HL-2A: e-BAE observed during ECRH

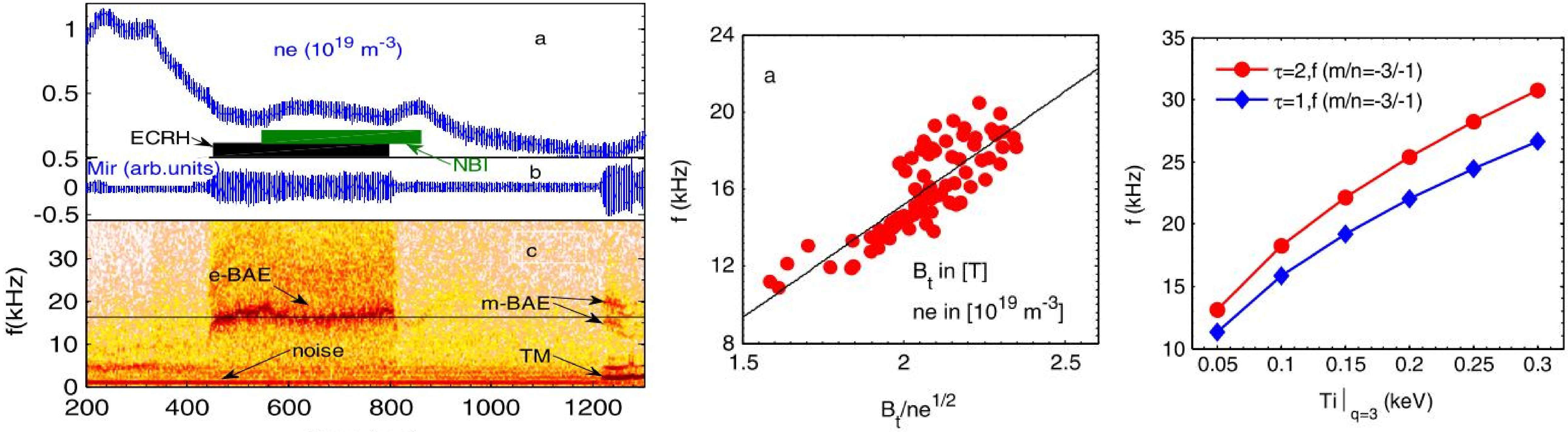

$$f_{\mathrm{BAE}} = (7/4 + T_{\mathrm{e}}/T_{\mathrm{i}})^{1/2}(2T_{\mathrm{i}}/m_{\mathrm{i}})^{1/2}/(2\pi R) + nf_{\phi}$$

- **β-induced Alfven eigenmode (BAE) excited by energetic electrons observed during ECRH.**
- **BAE is related not only with the population of energetic electrons, but also their energy and pitch angles.**

Chen W, PRL 105 185004 (2010)

AUG: Fast-ion (FI) loss induced by TAE and AC

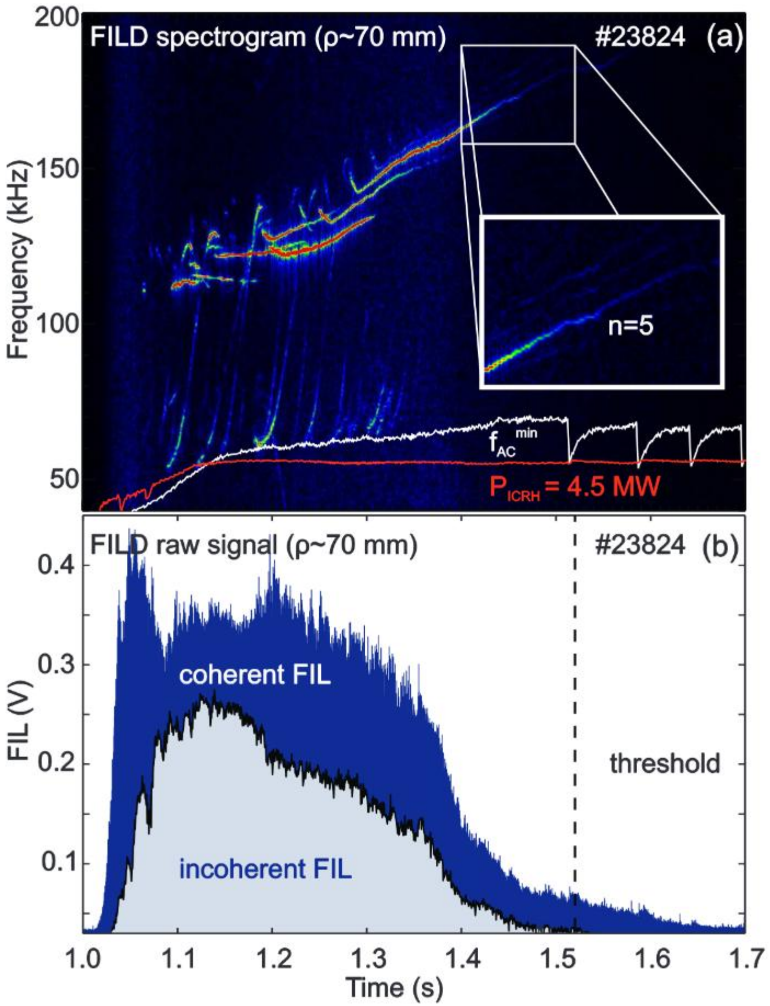

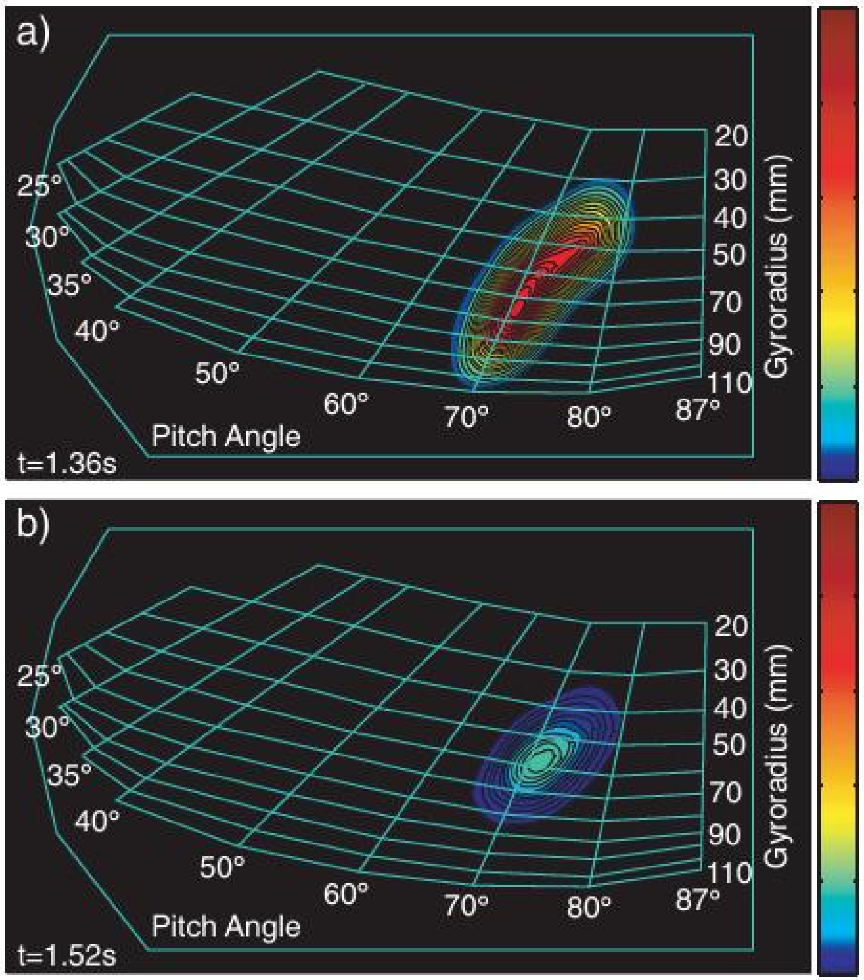

- **Heating and FI source: 4.5 MW on-axis ICRH (hydrogen minority $n_H/n_D \approx 5\%$) .**
- **TAEs and Alfven cascades (ACs) observed.**
- **FI loss mechnism by TAE and ACs investigated:**

  --Single TAE and AC induce convective FI loss.

  --Overlapping of TAE and ACs induces diffusive FI loss.

García-Muñoz et al., 2010 PRL, 104(18), 185002.

JET: MeV FI tail generated by three-ion scheme ICRF

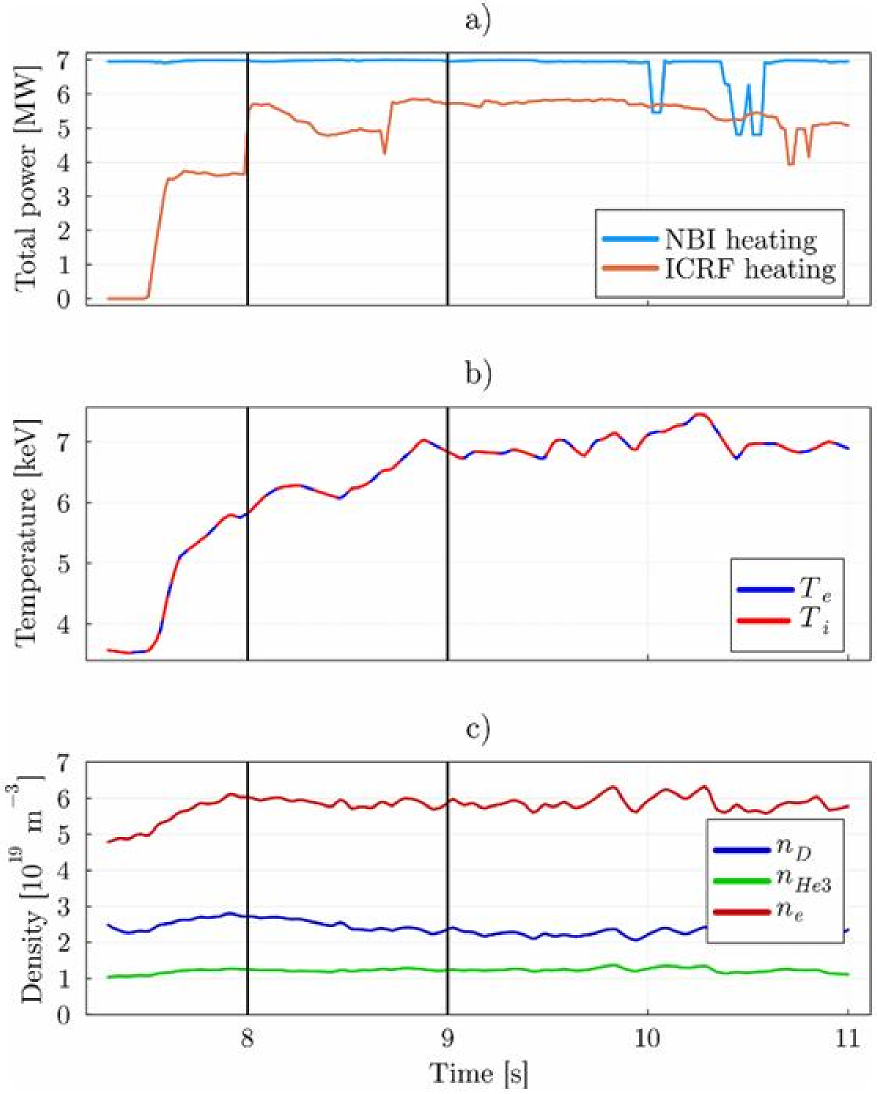

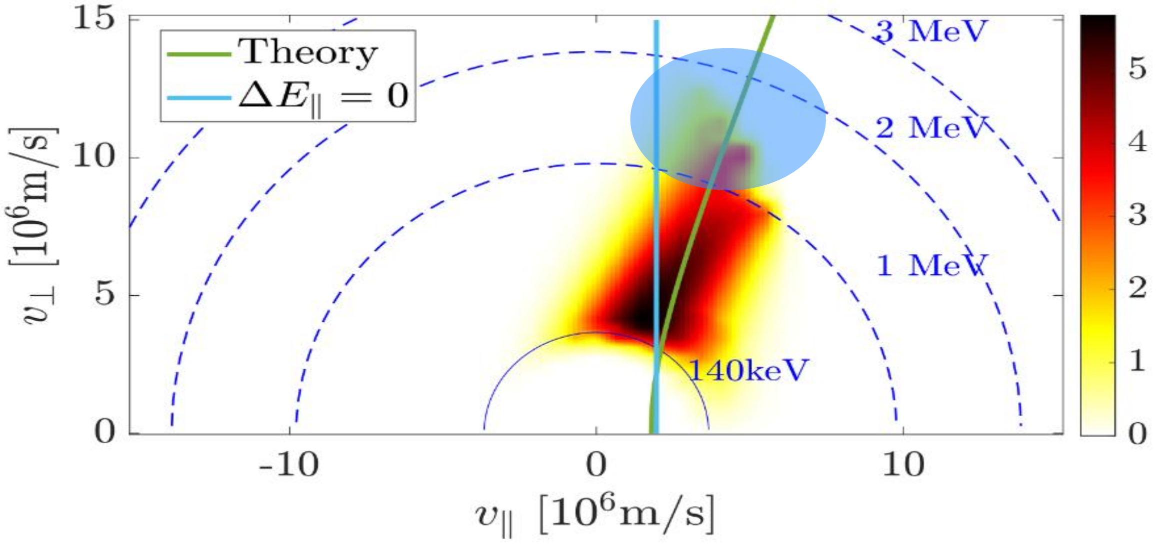

B.C.G. Reman 2025 NF 65 076007

D–D_{NBI}–^{3}He three-ion ICRF scheme:

- **Initial 110 keV D NBI population was accelerated to MeV energies (synergy of NBI and ICRH)**
- **Efficiently couples ICRF power to a selected ion population via Doppler-shifted absorption**

JET: Thermal ion confinement improved by MeV ions

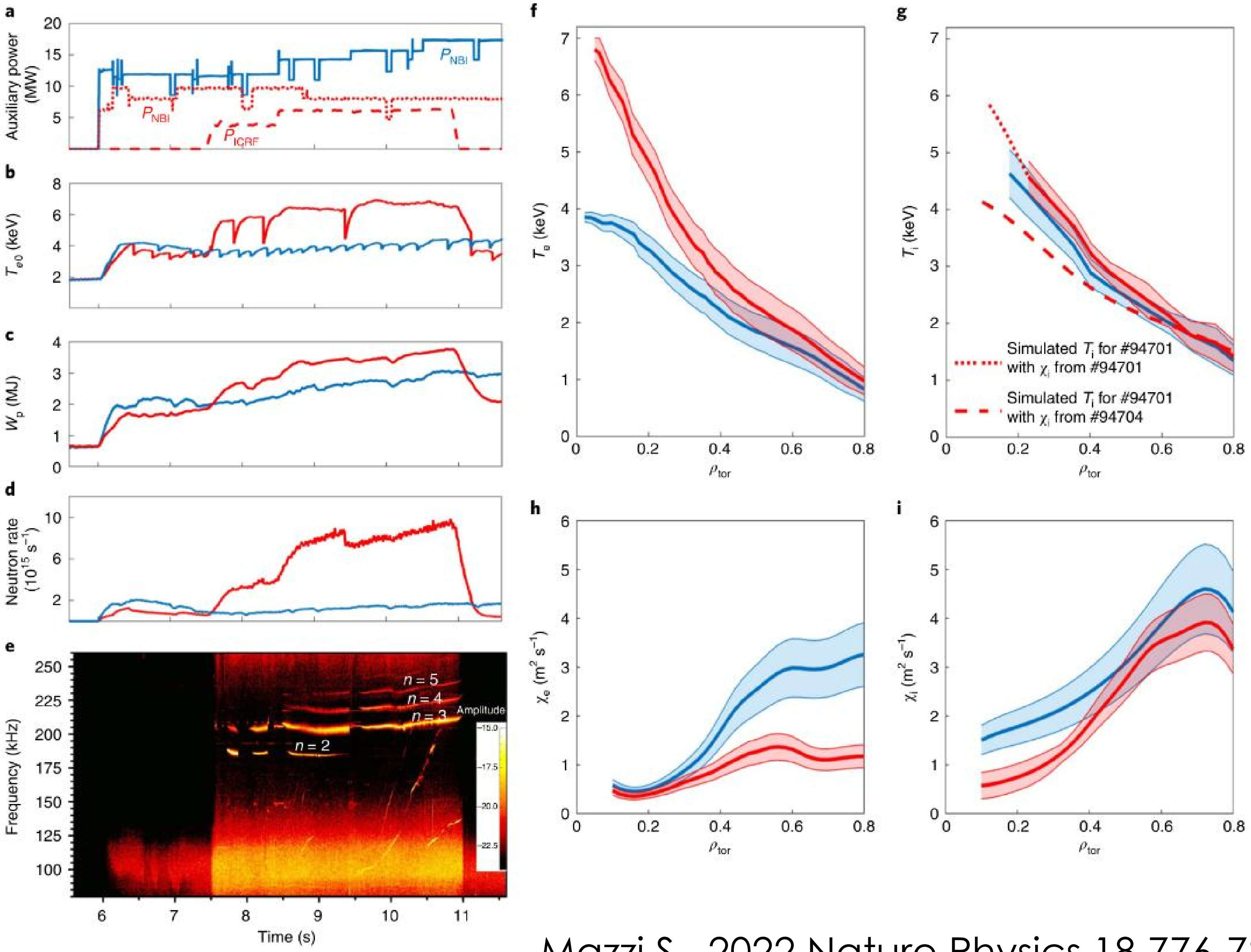

- Two shots with same operational conditions and P_{aux} = 14 MW
  Red: 94701, NBI+ICRH, ~ MeV ions
  Blue: 94704, NBI, ~100 keV ions
- Core ion heat diffusivity (TRANSP) drops by a factor of two by MeV ions.
- Arises from nonlinear coupling of AE to large-scale zonal flows, which shears ITG and suppresses radial ion heat transport.

Mazzi S., 2022 Nature Physics 18 776-782.

Outline

- Physical requirements for H&CD
- Overview of H&CD systems from experimental perspective
- Measurements of H&CD
- **Application in fusion experiments**
  - Profiles control and transport study
  - H-mode access
  - Fast-ion physics
  - Integrated control and scenario optimization
- Summary

JET: e-ITB real-time control by various heating

D Mazon, PPCF 44 (2002) 1087–1104

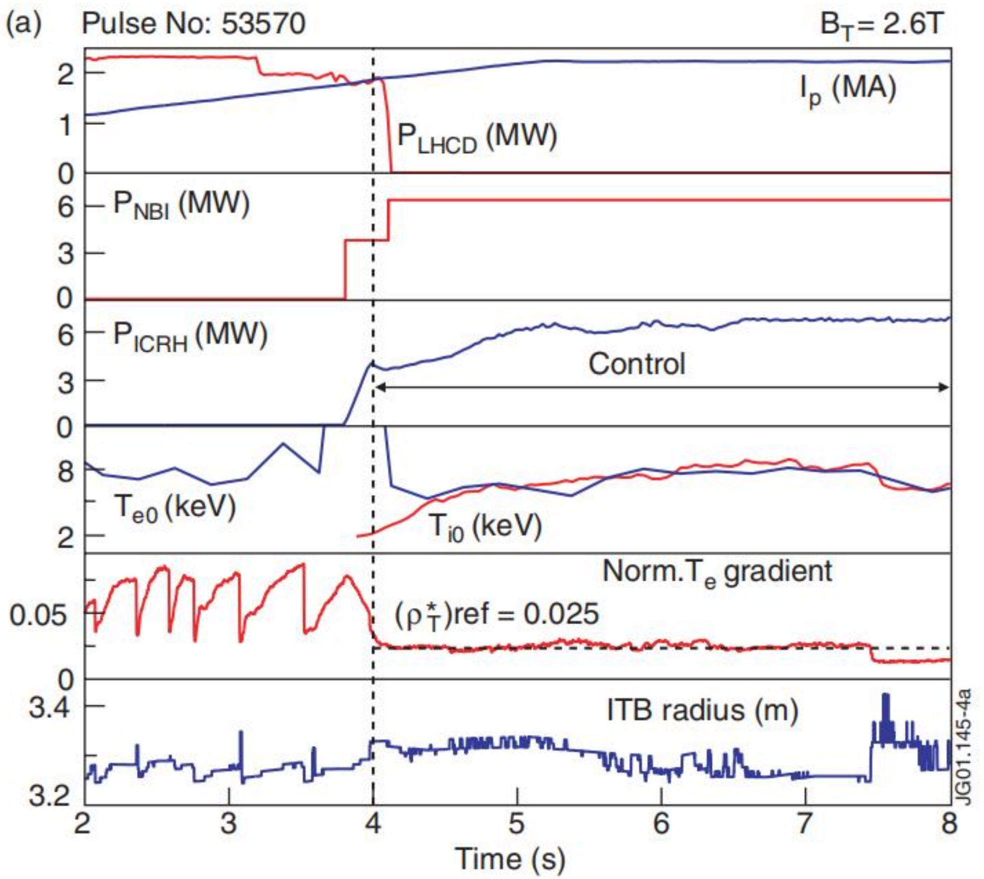

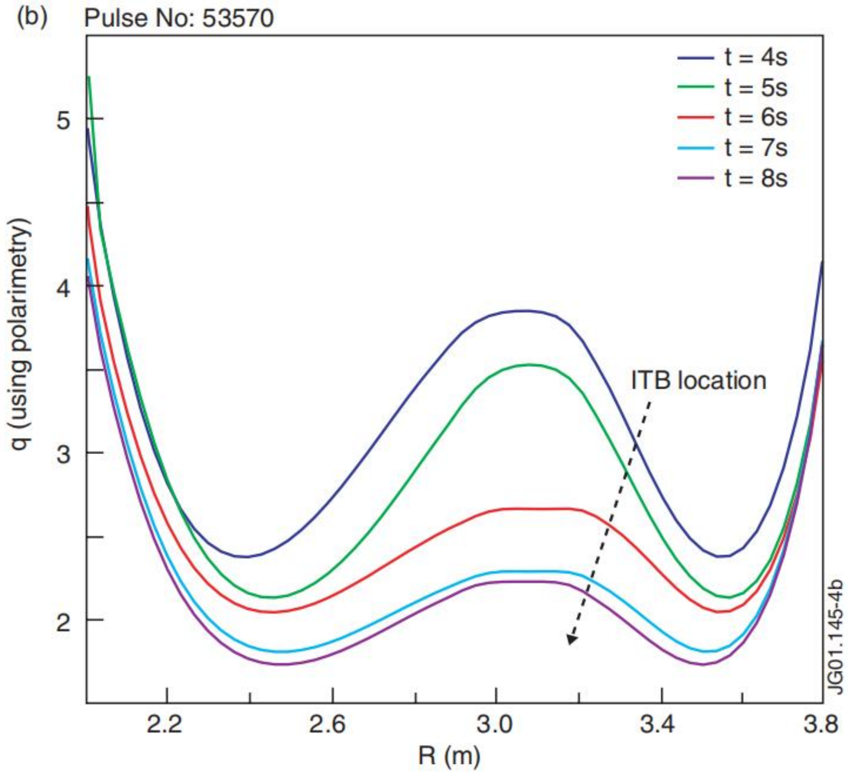

- LHCD induced strong negative magnetic shear (4s).

Control parameter: $\rho^*_T = \rho_s / L_{T_e} \propto \nabla T_e$

- During the high-power phase (4-8 s), the current profile relaxation governed by classical magnetic diffusion but slowed down by the intense heating. q is non-monotonic although LHCD is switched off.
- ITB remains located in the negative magnetic shear region.

JET: Hybrid scenario development

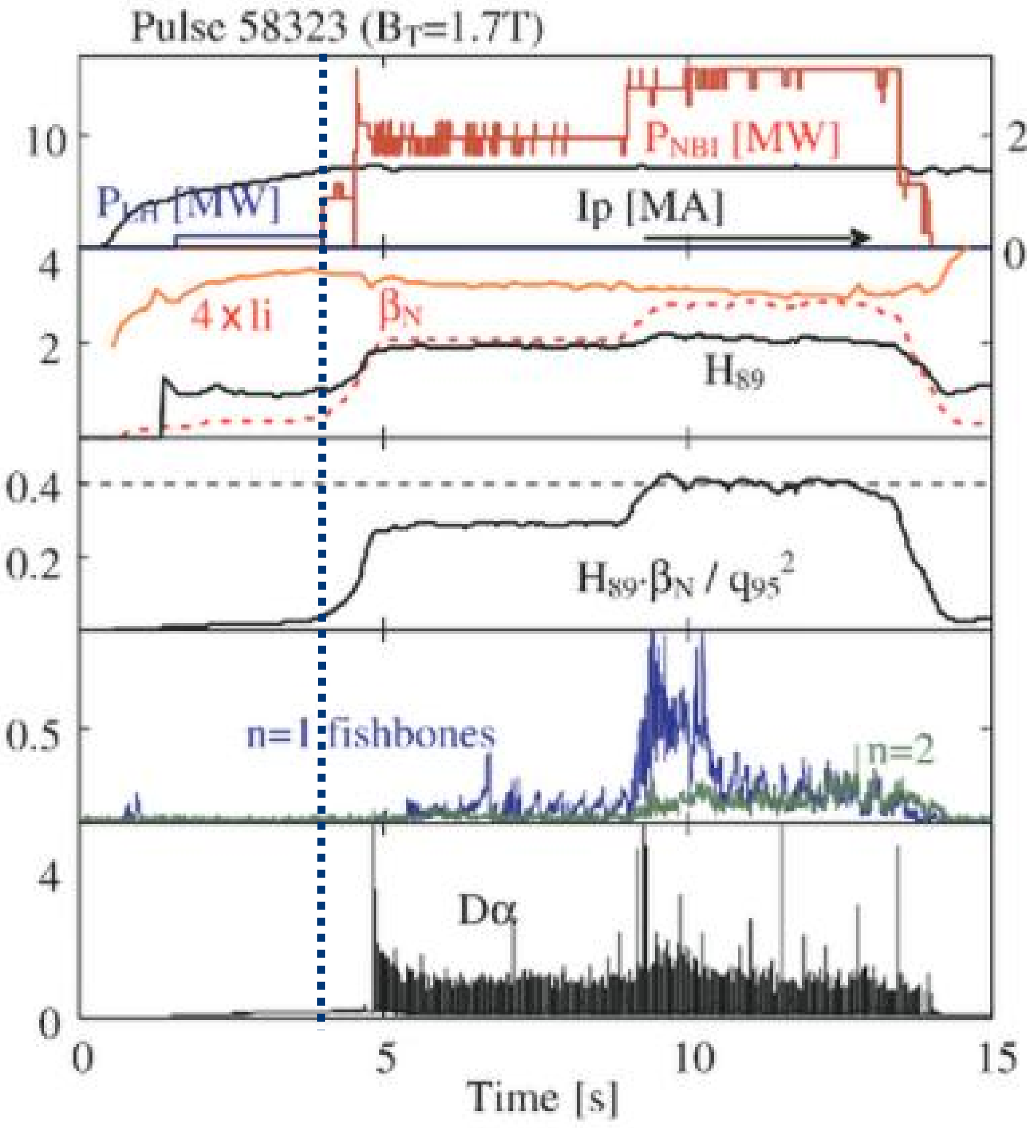

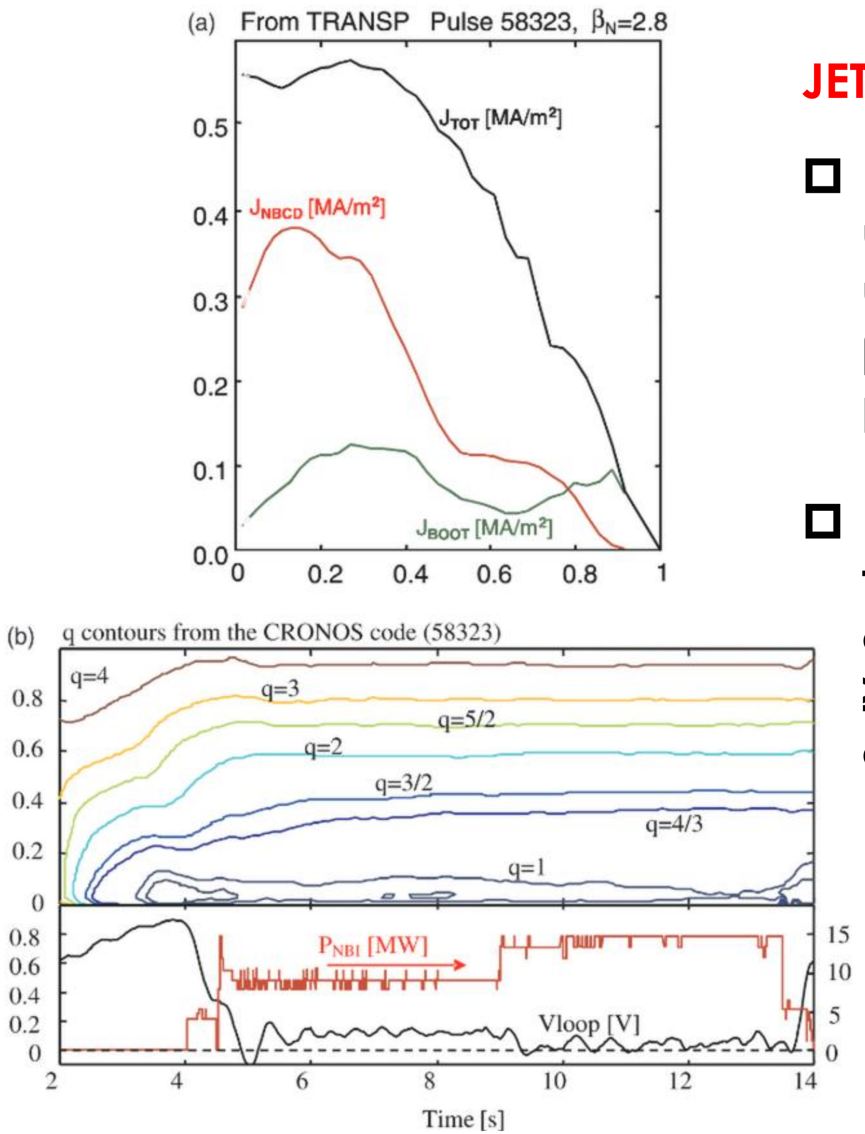

E. Joffrin 2005 NF 45 626

JET–AUG identity experiment

- LH power during ramp-up broadens q above unity, and NBI steps push β_N to 2.8 for high fusion performance.
- NBI-driven current, together with bootstrap current, then sustains $q_0 \geq 1$ for stationary operation.

JET: D-T scenario with optimized non-thermal fusion

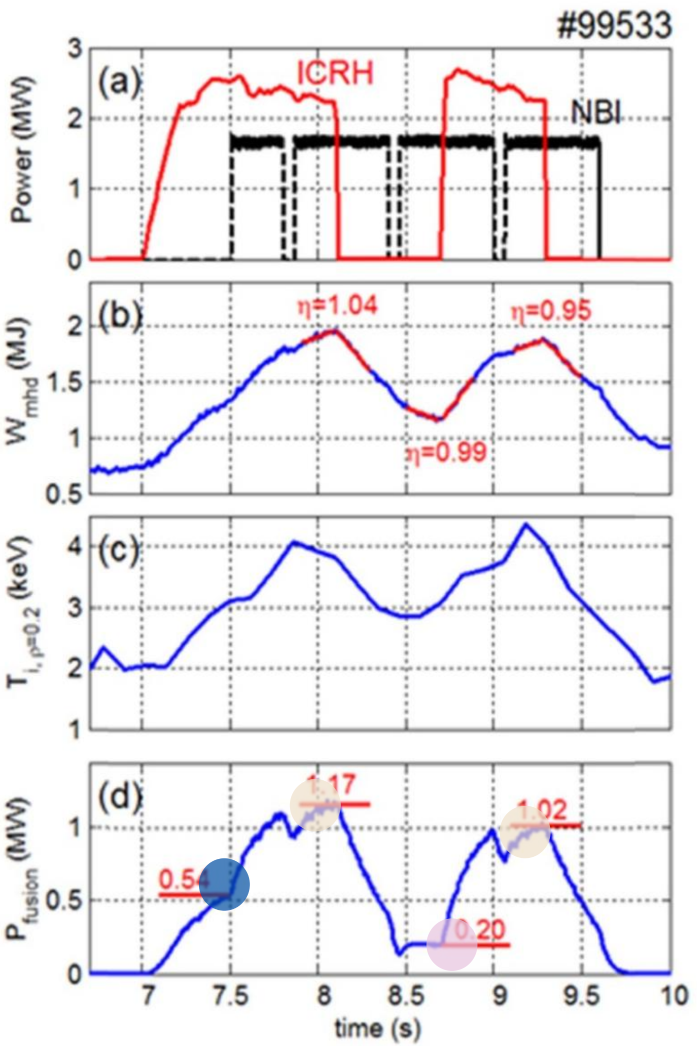

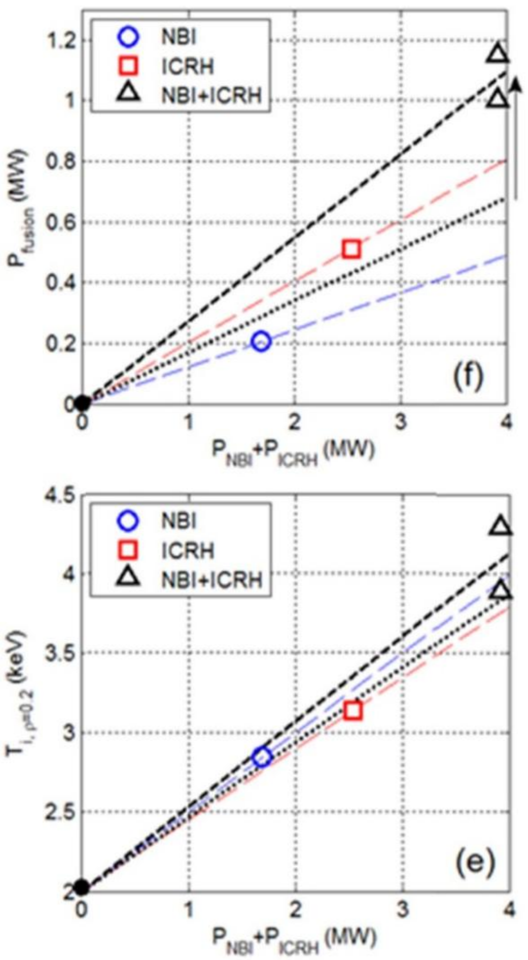

- L-mode, Bt=3.86 T, Ip=2.5 MA, tritium rich, D-NBI and fundamental-D ICRF.
- NBI-only (1.7 MW, 8.6 s): P_{fus}/P_{NBI}≈0.12, lower yield due to limited fast-ion population.
- ICRF-only (2.5 MW, 7.5 s): P_{fus}/P_{ICRF}≈0.2, shows efficient suprathermal D-tail generation.
- NBI+ICRF (2.5+1.7 MW, 8.1 s & 9.3 s): $P_{fus}/P_{NBI+CRH}$ = 0.27, the synergistic effect is ~35%.
- Synergistic effects have small impact on Ti

M. Maslov, 2023 NF 63 112002

Outline

- ☐ Physical requirements for H&CD
- ☐ Overview of H&CD systems from experimental perspective
- ☐ Measurements of H&CD
- ☐ Application in fusion experiments
  - ➢ Profiles control and transport study
  - ➢ H-mode access
  - ➢ Fast-ion physics
  - ➢ Integrated control and scenario optimization
- ☐ **Summary**

Summary

H&CD objectives	Experimental question	Diagnostics	Challenges
Heating/momentum toruqe	Power effectively absorbed?	Te, Ti, W_{dia}, V_{Φ}, neutron, ECE, CXRS	Losses, radiation, deposition
Current drive/q-profile	How much CD? Where?	MSE, loop voltage, equilibrium, HXR	Bootstrap/inductive separation
MHD control	Radial alignment	ECE, SXR, Mirnov, real-time q	Alignment accuracy and response time
Advanced Scenarios	q-profile controllable	MSE, transport modeling	Multiple actuators coupling
ITER-Relevant Operation	High-reliability, long-pulse operation?	Integrated diagnostics	High power handling, boundary control, materials, control systems

Summary

1. Heating and current drive are experimental actuators (profiles, turbulence and transport, rotation, stability, and fast particles), not merely auxiliary systems.

2. The key experimental questions are absorption, deposition, efficiency and controllability.

3. Future fusion devices require integrated H&CD control under reactor-relevant conditions.

Thanks for your attention！

JT-60U: Nearly full non-inductive CD by BS and NBCD

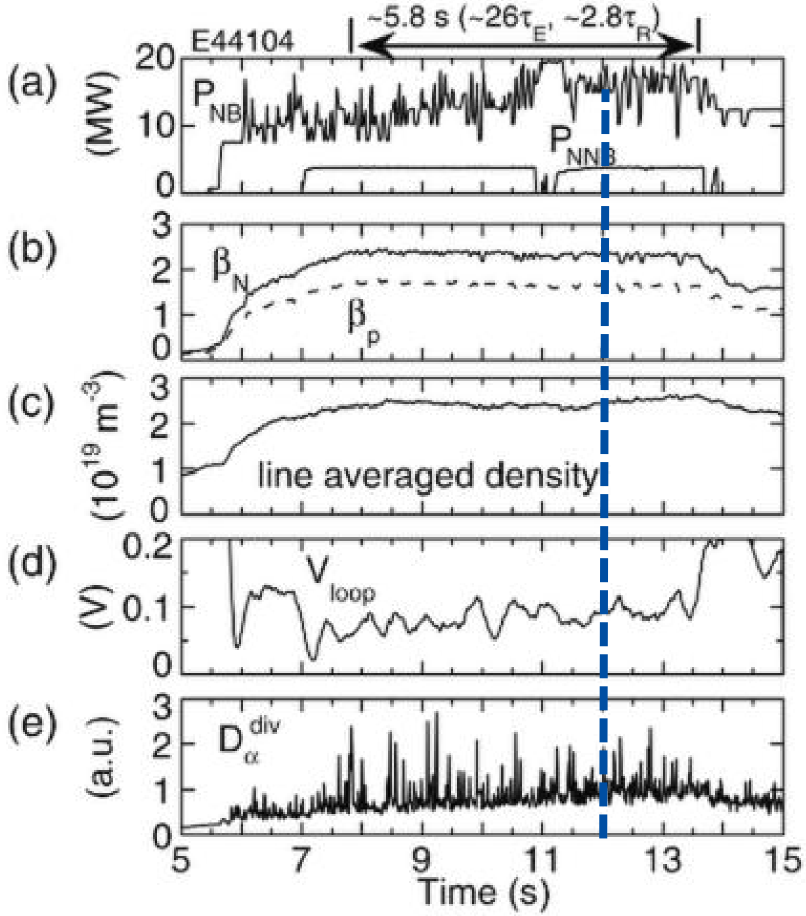

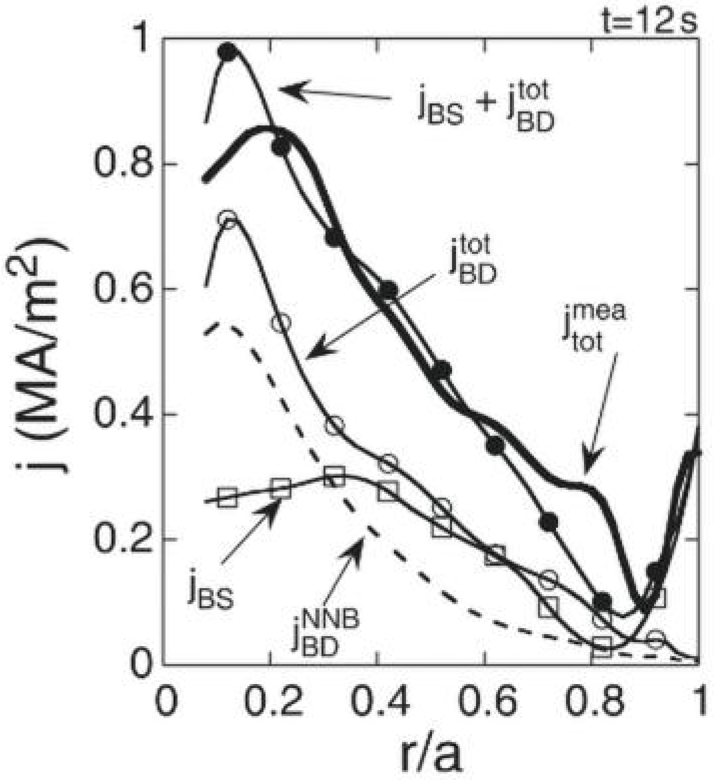

Y. Sakamoto 2005 NF 45 574

- **SS operation: high-β_p ELMy H-mode, f_{BS} ~ 45%, f_{BD} ~ 50%, H_{89} ~ 2.2 (HH_{98y2} ~ 1.0).**
- **J and P profiles reach SS condition.**
- **Duration ~ $26\tau_E$, ~ $2.8\tau_R$, limited by pulse length of negative-ion NBI.**